

## Chapter 2

# Where Does Mercury in the Arctic Environment Come From, and How Does it Get There?

COORDINATING AUTHORS: JOHN MUNTHE, MICHAEL GOODSITE

CO-AUTHORS: TORUNN BERG, JOHN CHÉTELAT, AMANDA COLE, ASHU DASTOOR, TOM DOUGLAS, DOROTHY DURNFORD, MIKE GOODSITE, ROBIE MACDONALD, DEREK MUIR, JOHN MUNTHE, PETER OUTRIDGE, JOZEF PACYNA, ANDREW RYZHKOV, HENRIK SKOV, ALEXANDRA STEFFEN, KYRRE SUNDSETH, OLEG TRAVNIKOV, INGVAR WÄNGBERG, SIMON WILSON

DATA CONTRIBUTORS: ALEX POULAIN, JESPER CHRISTENSEN

### 2.1. Introduction

Very little of the Hg present in the Arctic is derived from pollution sources within this region; most is transported in from anthropogenic and natural sources outside the Arctic (AMAP, 2005). Previous AMAP assessments (AMAP, 1998, 2005) have discussed in detail the atmospheric, oceanic, riverine and terrestrial pathways by which mercury is transported into the Arctic. As a result, these pathways are only considered in relation to specific issues in this report. However, it remains the case that the Arctic is intimately and inextricably linked by these pathways to the global Hg cycle.

This chapter begins by summarizing recent information about Hg in the global environment and, specifically, about the global Hg reservoirs that interact with the regional Arctic environment, essentially through the atmosphere and oceans. This is followed by an introduction to the physical linkages between the global and regional environmental 'reservoirs', and the chemical species of Hg involved. To provide a conceptual linkage to Chapter 3, an ordered perspective is also placed on the important processes that deliver transported Hg to the Arctic ecosystems. For each process, the reader is directed to corresponding discussion in subsequent sections of this chapter and in Chapter 3.

#### 2.1.1. The Arctic in a global setting

A recent model of the Hg cycle in the contemporary global environment is summarized in Figure 2.1. It is clear that surface soils contain by far the largest Hg reservoir. However, with the exception of soils present in the Arctic itself, global soil Hg only interacts with the Arctic on meaningful time scales indirectly through the atmosphere and ocean. Sunderland and Mason (2007) estimated that about 134 000 t of Hg presently reside in the upper oceans and about 5600 t in the atmosphere. These reservoirs include pollution-related increases of about 25% in the upper oceans and 300% to 500% in the atmosphere, relative to the pre-industrial period. The most recently available (2005) estimates of global anthropogenic Hg emissions to air are discussed in Section 2.2.

The global model shows that there are large air-sea Hg exchanges that make it difficult to determine the net direction of flux. The upper global oceans (top 1500 m) contain about one third of the total ocean inventory but clearly there is the suggestion of vigorous processes (particle flux, deep-water formation) that remove Hg from the surface to deep oceans. Another important point is that almost all of the Hg transported from land to oceans via rivers becomes stored in estuaries and on continental shelves. From an Arctic perspective, the most important pathways for Hg transport to the Arctic involve the upper oceans and the atmosphere, because these reservoirs directly and relatively rapidly interact with the corresponding

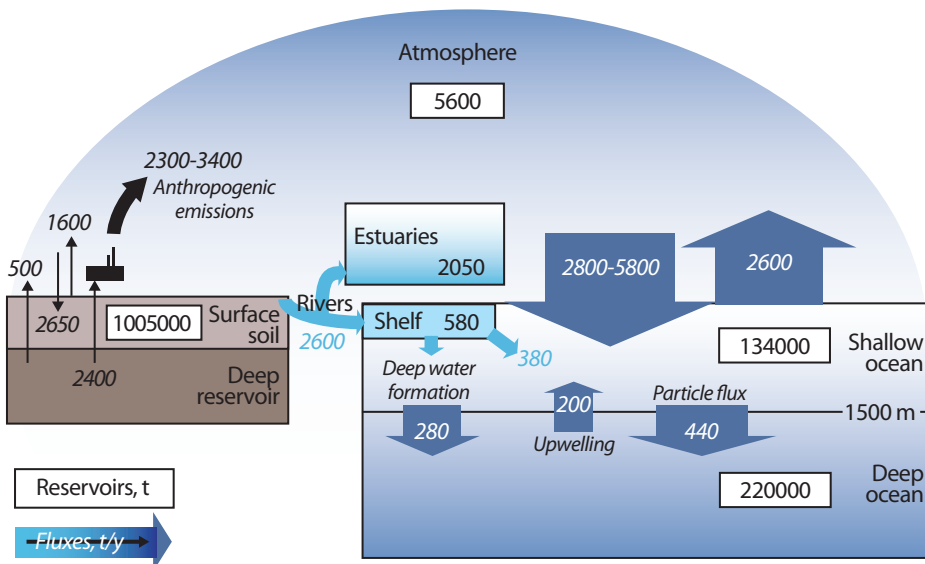


Figure 2.1. A global model of mercury inventories in present-day air, ocean and soil reservoirs, and the fluxes which indirectly or directly contribute to mercury levels in the Arctic. Adapted from Sunderland and Mason (2007).

reservoirs in the Arctic over biologically relevant time frames (Outridge et al., 2008).

One important conclusion from the air-ocean modeling work is that, on average, the global oceans have not yet reached equilibrium with the present-day atmospheric Hg levels. This means that average seawater Hg concentrations are likely to increase slowly for periods of decades to several centuries, even if there is no further increase in atmospheric Hg levels (Sunderland and Mason, 2007). Regional differences in seawater Hg trends are expected, with the time taken to reach equilibrium predicted to differ as a result of varying circulation patterns, water residence times, and proximity to regions of industrial activity. For example, mid-range regional estimates for the North Atlantic Ocean suggest a stable or declining future trend rather than an increase. The response time of the North Atlantic above 55° N to changes in atmospheric Hg concentrations is estimated to be 50 to 600 years, whereas in the North Pacific Ocean it may take 500 to 700 years for Hg concentrations to reach steady-state. Surface waters will naturally respond more rapidly than deep and intermediate water layers; for example, the surface Atlantic Ocean may reach equilibrium in just 10 to 30 years. More recent studies have not changed the seminal conclusions of Mason et al. (1998) that the biogeochemical cycling of Hg in the ocean is dominated by air-sea exchange at the sea surface, with removal of Hg to deep ocean sediments being analogous to that of carbon (i.e., only a small fraction of the Hg taken up by mixed-layer particulate matter is buried in deep water sediments). What is still clear is that the external inputs from different oceans to the Arctic Ocean will vary partly because of systematic differences in circulation patterns, residence times, and other abiotic and biotic processes.

The extent to which changes in these global reservoirs affect Hg levels in the Arctic environment depends on the degree of connectivity between the reservoir and the Arctic, which is a function of the speed of lateral transfer into the Arctic and the average residence time of Hg in the various environmental compartments and media. The amount of Hg present from natural sources within the Arctic (see Section 2.3) is also a factor, as the relative contribution of the external inputs to each environmental medium is greater if the local 'background' contamination is low and vice versa. The average residence times for Hg in the global atmosphere and upper oceans at the present time, which can be derived from the Sunderland and Mason (2007) model, are about 0.7 and about 27 years, respectively. Lateral transfer is likely to be significantly slower for seawater (of the order of centimetres per second) than for air (of the order of metres per second). However, given the long residence time of Hg in seawater it is likely that changes in global upper ocean and atmospheric Hg will both affect their Arctic counterparts but over differing time scales – relatively rapidly for the atmosphere and slowly for seawater. Recent best estimates of the net total Hg fluxes currently reaching the Arctic Ocean from global reservoirs via different pathways (ocean currents, atmosphere, rivers, coastal erosion), and the corresponding sizes of Hg reservoirs in the Arctic, are presented in Section 2.4.

### 2.1.2. Mercury processing in the Arctic environment

Inorganic Hg(II) is the key Hg 'feedstock' from which the more toxic and bioavailable monomethyl-Hg (MeHg) is formed in surficial environments (oceans, lakes, soils). One important difference between the atmospheric and aquatic transport pathways (see Figure 3.3) is that the dominant form of Hg present in the atmosphere and hence transported into the Arctic via the atmosphere is gaseous elemental Hg (GEM, Hg(0)). This must undergo chemical transformation to inorganic Hg(II) in the atmosphere in order for it to be deposited to Arctic surface environments. Unreacted GEM is simply transported out of the Arctic again by air mass movements. In contrast, Hg inputs via oceans, rivers, and coastal erosion already comprise mainly inorganic Hg(II), as well as small amounts of methylated Hg(II) and dissolved gaseous Hg(0), because of transformations that occurred in these reservoirs before the Hg reached the Arctic environment.

Because Arctic atmospheric transformations of Hg(0) to Hg(II) form such an integral part of the answer to the 'how does it get there' component of the main question addressed in this chapter, these transformations are discussed in detail here. The subsequent transformations, dynamics, and fate of Hg in Arctic waters, soils, sediments, and food webs are addressed in Chapter 3. As marine food webs (and especially marine mammals) appear to be the major exposure route of northern peoples to Hg (AMAP, 2009b; see also Chapter 8), the behavior and fate of Hg in the marine environment is a particular focus for Chapter 3.

Recent findings on Arctic atmospheric speciation and transformation of Hg, including wet and dry deposition processes and atmospheric mercury depletion events (AMDEs), are described in Section 2.5. The extent to which current understanding of these processes permits modeling to describe and quantify the fluxes of atmospheric Hg in the Arctic is evaluated in Section 2.6. The atmospheric Hg(II) is deposited into the upper ocean, into snowpacks, or into soil and freshwater environments, where it mixes with Hg(II) and other Hg species from global oceanic and local terrestrial geogenic sources (see Figure 3.3; Section 3.2). Thereafter, changes in chemical speciation occur via physical, chemical, and biological processing in marine, freshwater, and terrestrial environments, and result predominantly in three important forms of Hg: monomethyl mercury (MeHg), particulate-associated Hg(II) (Hg<sub>p</sub>) and gaseous Hg(0). These Hg species are moved around, transformed into other Hg species, or recycled by internal processes in each environmental medium. Methylation of inorganic Hg(II) to MeHg (Section 3.3), and its uptake into Arctic food webs (Section 3.4), are two key steps in the exposure route between environmental Hg and Hg in human food chains. Mercury uptake into food webs is influenced by trophic processes that can affect the efficiency of MeHg transfer from lower to upper levels of food webs (Section 3.5), as well as by effects on Hg bioavailability by co-occurring materials such as organic carbon (Section 3.7). Ultimately, Hg is removed from the biologically-active Arctic environment to long-term storage in various archives such as ocean sediments, soils, and glacial ice (Section 3.8), or by transport out of the Arctic in air and seawater (see Figure 2.2).

## 2.2. What are the current rates of global anthropogenic emissions of mercury to air?

### 2.2.1. Global anthropogenic mercury emissions to air in 2005

Quantifying sources of Hg and its transport via atmospheric and aquatic pathways is fundamental to understanding the global fluxes and contamination of ecosystems by this metal. Due to the relatively long atmospheric-lifetime of GEM, Hg can be transported to the Arctic via the atmosphere from sources around the globe. Consequently, an assessment focusing on Arctic contamination needs to consider global emissions of Hg. Understanding global Hg emissions is also critical for the development of relevant and cost-efficient strategies aimed at reducing the negative impacts of this global pollutant. Emission inventories provide important input data for several types of atmospheric chemical-transport and source-receptor models that can provide information on Hg distribution and deposition rates. This section focuses on primary anthropogenic emissions to the atmosphere. For a full description of the atmospheric cycling of Hg, information on natural emissions as well as re-emissions of Hg deposited to land and water need to be considered and are presented in Sections 2.3 to 2.6.

The need for information on global emissions of Hg to the atmosphere to support work on Arctic Hg assessments has led to a strong connection between AMAP assessment activities and work by groups engaged in producing these global inventories. As a result, past AMAP assessments have integrated information on global anthropogenic emission inventories produced for the nominal years 1990 (AMAP, 1998) and 1995 and 2000 (Pacyna and Pacyna, 2002; AMAP, 2005). Most recently, an inventory of the global anthropogenic Hg emissions for 2005 (the '2005 v5' inventory) was prepared in a joint AMAP/UNEP project in 2008. Details on the methods, data sources and other information are reported by AMAP/UNEP (2008) and Pacyna et al. (2010a). Further work on the 2005 inventory was undertaken as part of the present assessment (see Section 2.2.2), resulting in the '2005 v6' inventory. The 2005 global

anthropogenic emissions inventory was also used as a basis for developing some first order 'scenario' emissions inventories for 2020 (AMAP/UNEP, 2008). The scenario inventories and modeling work based on these inventories are presented in Chapter 7.

#### 2.2.1.1. Global emissions to air by industrial sectors

The largest anthropogenic emissions of Hg to the global atmosphere occur as a by-product of the combustion of fossil fuels, mainly coal in power plants and industrial and residential boilers. As much as 60% of the total emission of roughly 1450 tonnes of Hg emitted from 'by-product' sector sources, and 46% of the roughly 1921 tonnes of Hg emitted from all anthropogenic sources worldwide in 2005, came from the combustion of fossil fuels for energy and heat production (Table 2.1). Emissions of Hg from coal combustion are between one and two orders of magnitude higher than emissions from oil combustion, depending on the country. Some uncertainties remain about the magnitude of Hg emissions from natural gas and oil processing. Mercury is present in some natural gas deposits but is removed before distribution to avoid corrosion of aluminum equipment in the processing plants. The final fate of this Hg, and the potential emissions of Hg from crude oil processing and combustion, warrants further evaluation. Various factors affect the emission of Hg to the atmosphere during combustion of fuels. The most important are the Hg content of the coal and the type and efficiency of control equipment that can remove Hg from exhaust gases (as well as, naturally, the amount of fuel combusted).

Emissions from non-ferrous and ferrous metal industry (excluding Hg and gold production) are estimated to contribute about 10% to total anthropogenic Hg emissions. The content of Hg in ores varies substantially from one ore field to another (e.g., Pacyna, 1986; UN ECE, 2000) as does the Hg content in scrap metal. The Hg emissions from primary metal production (using ores) are between one and two orders of magnitude higher than the Hg emissions from secondary smelters (with scrap as the main raw material), depending on the country.

Table 2.1. Estimated global anthropogenic emissions of mercury to air in 2005 from various sectors (revised from AMAP/UNEP, 2008).

Sector	Emissions in 2005 <sup>a</sup> , tonnes	Percentage contribution of total emissions to air
Coal combustion in power plants and industrial boilers	498 (339-657)	26
Residential heating / other combustion	382 (257-506)	20
Artisanal and small-scale gold production	323	17
Cement production	189 (114-263)	10
Non-ferrous metals (Cu, Zn, Pb)	132 (80-185)	7
Large-scale gold production	111 (66-156)	6
Other waste	74	4
Pig iron and steel, secondary steel	61 (35-74)	3
Waste incineration	42	2
Chlor-alkali industry	47 (29-64)	2
Dental amalgam (cremation) <sup>b</sup>	27	1
Other	26	1
Mercury production	9 (5-12)	0.5
Total	1921	

<sup>a</sup> Represents best estimates: estimate (uncertainty interval), or conservative estimate (no associated range). See AMAP/UNEP (2008) for discussion on uncertainties; <sup>b</sup> does not include other releases from production, handling, use and disposal of dental amalgam.

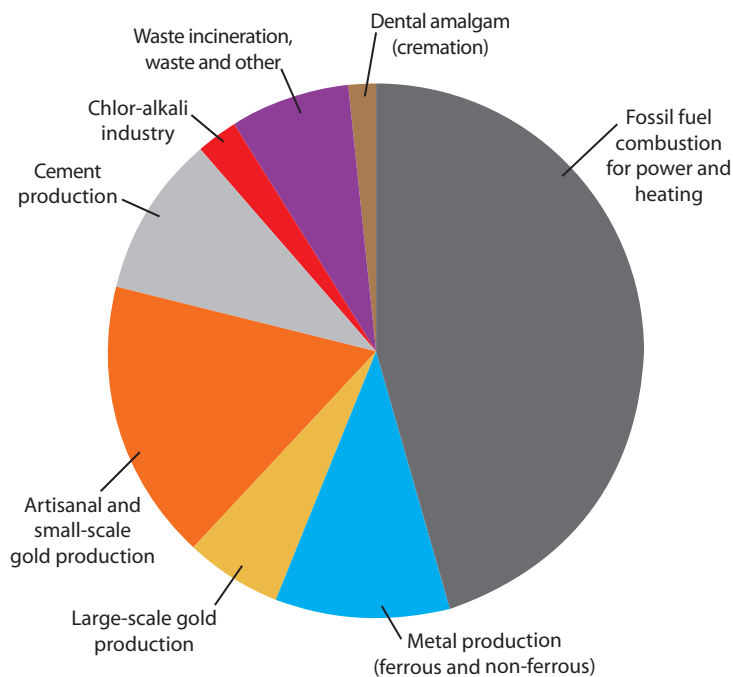


Figure 2.2. Proportion of global anthropogenic emissions of mercury to air in 2005 from various sectors. Source: revised after AMAP/UNEP (2008).

Pyro-metallurgical processes in primary production of non-ferrous metals, employing high temperature roasting and thermal smelting, emit Hg and other raw material impurities mostly to the atmosphere. Non-ferrous metal production with electrolytic extraction is more responsible for risks of water contamination.

Among various steel making technologies the electric arc process produces the largest amounts of trace elements, and their emission factors are about one order of magnitude higher than those for other techniques, for example, basic oxygen and open hearth processes. However, the major source of atmospheric Hg related to the iron and steel industry is the production of metallurgical coke.

The fuel-firing kiln system and the clinker-cooling and handling system are responsible for emissions of Hg in the cement industry. This industry contributes about 9.8% of the total anthropogenic Hg emissions (and 13% of 'by-product' Hg emissions) on a global scale. The content of Hg in fuel, limestone and other raw materials used in the kiln and the type and efficiency of control equipment are the main parameters affecting the size of Hg emissions.

Industrial (large-scale) gold production using Hg technology is another source of Hg to the atmosphere, contributing about 6% to the global Hg emissions.

The use of the mercury cell process to produce caustic soda in the chlor-alkali industry has decreased significantly over the past 15 years worldwide (www.eurochlor.org). The atmospheric chlor-alkali Hg emissions of 47 tonnes in 2005 account for less than 10% of Hg used in this production process and about 2.5% of the total anthropogenic Hg emissions worldwide. Major points of Hg release in the mercury cell process of chlor-alkali production include: by-product hydrogen stream, end box ventilation air, and cell room ventilation air. For long-term avoidance of emissions, safe storage of Hg-containing waste from these steps is required.

Mercury production for industrial uses contributes just over 0.5% to global Hg emissions.

The global product-related emissions of Hg (including all major uses of Hg in products) were estimated to be around 125 tonnes (6.5%) for the conservative estimate in the AMAP/UNEP (2008) study (Table 2.1). This estimate has subsequently been revised to 142 tonnes (7.4%). It is noteworthy that according to these calculations, around 30% of the product-related Hg emissions arises from waste incineration and another 52% from landfill waste.

Summing the Hg emissions from 'by-product' sectors, product use, cremation and artisanal / small-scale mining, results in a global inventory of Hg emissions to air from anthropogenic sources for 2005 of about 1920 tonnes. Table 2.1 and Figure 2.2 summarize the emissions attributed to various anthropogenic activities. The low- and high-end estimates are based on the uncertainties in emission estimates for the different sectors.

### 2.2.1.2. Emissions by geographical region

The combined global anthropogenic atmospheric Hg emissions inventory for by-product sectors, product use, cremation and artisanal mining of about 1920 tonnes for 2005 can be divided between the continents as summarized in Figure 2.3. From the compiled inventory data, it is possible to rank the countries by their emissions (see Figure 2.4). The sector-breakdown of emissions from the ten largest emitting countries is presented in Figure 2.5.

The Asian countries contributed about 65% to the global Hg emissions from anthropogenic sources in 2005, followed by North America and Europe. This pattern is similar if by-product emission sectors only are considered. Russia, with its contribution of about 4% to global emissions is considered separately due to its territories in both Europe and Asia.

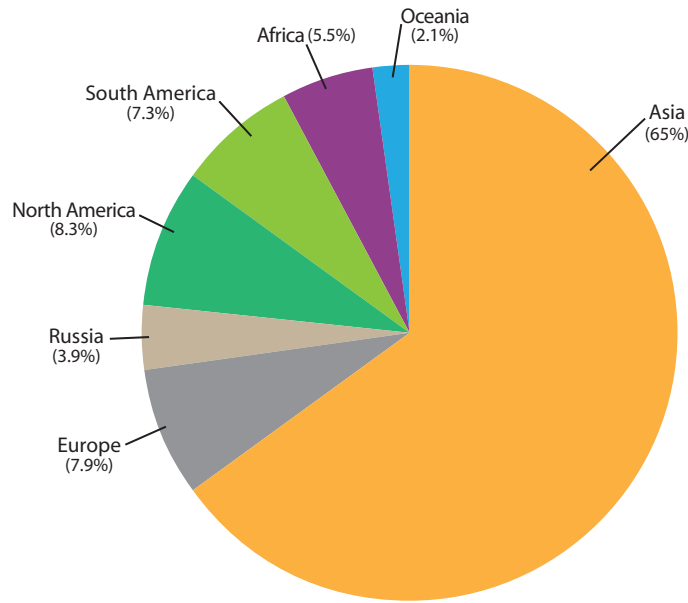


Figure 2.3. Proportion of global anthropogenic emissions of mercury to air in 2005 from different regions. Source: revised after AMAP/UNEP (2008).

Combustion of fuels to produce electricity and heat is the largest source of anthropogenic Hg emissions in Europe, North America, Asia, and Russia, and is responsible for about 35% to 50% of the anthropogenic emissions in Oceania and Africa. However, in South America, artisanal and small-scale gold mining (ASGM) is responsible for the largest proportion of the emissions (about 60%). Relatively large Hg emissions from ASGM in some Asian countries, as well as several countries in South America, explain why countries such as Indonesia, Brazil and Colombia appear in the top ten ranked Hg emitting countries,

whereas if by-product emissions sectors alone are considered, no South American countries are represented and all other countries listed have a high degree of industrial development.

China is the largest single emitter of Hg worldwide, by a large margin. Power plant emissions are an important part of the total combustion emissions of Hg in China although the ongoing restructuring and improved emission control of air pollutants in the Chinese power sector may have reduced the importance of this sector in recent years. Equally significant are emissions from combustion of poor quality coal mixed with various kinds

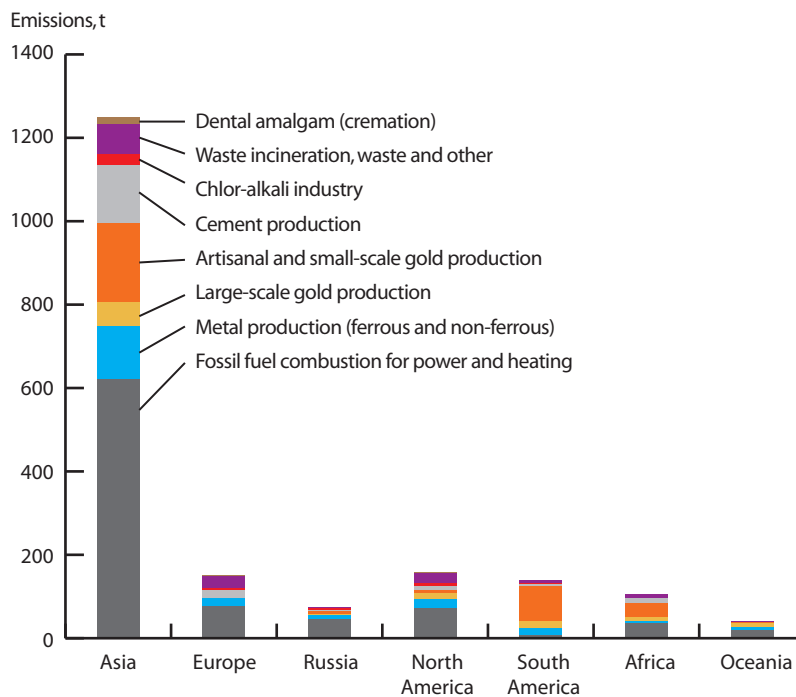


Figure 2.4. Global anthropogenic emissions of mercury to air in 2005 from different continents by sector. Source: revised after AMAP/UNEP (2008).

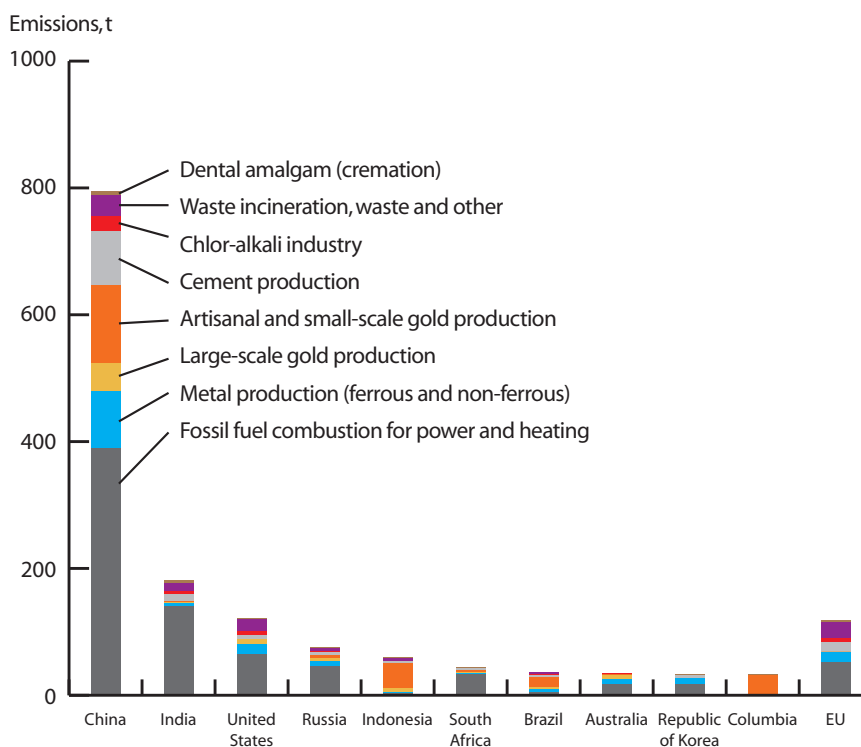


Figure 2.5. Emissions of mercury to air in 2005 from various anthropogenic sectors in the ten largest emitting countries. Source: revised after AMAP/UNEP (2008).

of wastes in small residential units to produce heat and cook food in rural areas. With estimated by-product sector emissions exceeding 600 tonnes, China contributes about 40% to the global Hg by-product emissions, and this contribution may be even higher because Hg emission factors for non-ferrous metal production in China may be underestimated. China also has significant emissions from ASGM.

Together, China, India, and the United States, are responsible for about 60% of the total global Hg emissions from by-product sectors (about 895 out of 1450 tonnes), and a similar percentage of the total estimated global emission inventory for 2005 (1095 out of 1920 tonnes).

### 2.2.2. Global emission trends 1990 to 2005

The 2005 (v5) global inventory of anthropogenic Hg emissions to air, described by AMAP/UNEP (2008) and summarized by UNEP (2008), was the most comprehensive such inventory published to date. Unlike previous global inventories, which essentially only addressed 'by-product' Hg emissions from main energy production and industrial sectors, the 2005 inventory also included estimates of emissions associated with a number of 'intentional-use' sectors, including artisanal and small-scale gold production.

The 2005 inventory was produced using a generally similar approach to that employed to compile (on the basis of 'by-product' sectors) Hg emission inventories for the nominal years 1990, 1995 and 2000 (Pacyna and Pacyna, 2002; Pacyna et al., 2006, 2010a; AMAP/UNEP, 2008), namely by combining reported national emissions for specific sectors with expert estimates for the remaining countries for the same range of sectors. The expert estimates were obtained using information on production and consumption of raw materials in relevant

industries, in combination with applicable emission factors. However, since each inventory was compiled independently at about five-year intervals, the underlying source data used varied in terms of their sources, availability and quality. Furthermore, emission factors and the assumptions regarding technologies employed changed as knowledge was improved.

Each of the four available global inventories has also been geospatially distributed (gridded), again using similar but not identical methods (see Pacyna et al., 2003; Wilson et al., 2006; AMAP/UNEP, 2008). These inventories have been used to model the atmospheric transport of Hg, and investigate geographic source-receptor relationships (see Dastoor and Larocque, 2004; Christensen et al., 2004; Travnikov, 2005; AMAP/UNEP, 2008; Dastoor et al., 2008). Results of modeling using the 1990, 1995, 2000, and 2005(v6) global anthropogenic emissions inventories described here, and the 2005(v5) inventory presented in the previous section, are discussed in Section 2.6.

Figure 2.6 presents the global distribution of anthropogenic atmospheric emissions of Hg in 2005, following application of the geospatial distribution methodology described by Wilson et al. (2006) and Pacyna et al. (2010a) to the global anthropogenic (2005v5) inventory (AMAP/UNEP, 2008).

The AMAP/UNEP (2008) report included a preliminary discussion of the general trends in global emissions as implied from comparing the available 1990, 1995, 2000 and 2005 inventories. However, such a comparison may be compromised by methodological differences between years.

Consequently, and as part of its 2010 assessment of Hg in the Arctic, AMAP undertook a re-analysis of the 1990 to 2005 global Hg inventories in an attempt to prepare a series of more comparable historical emission inventories.

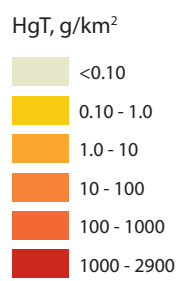
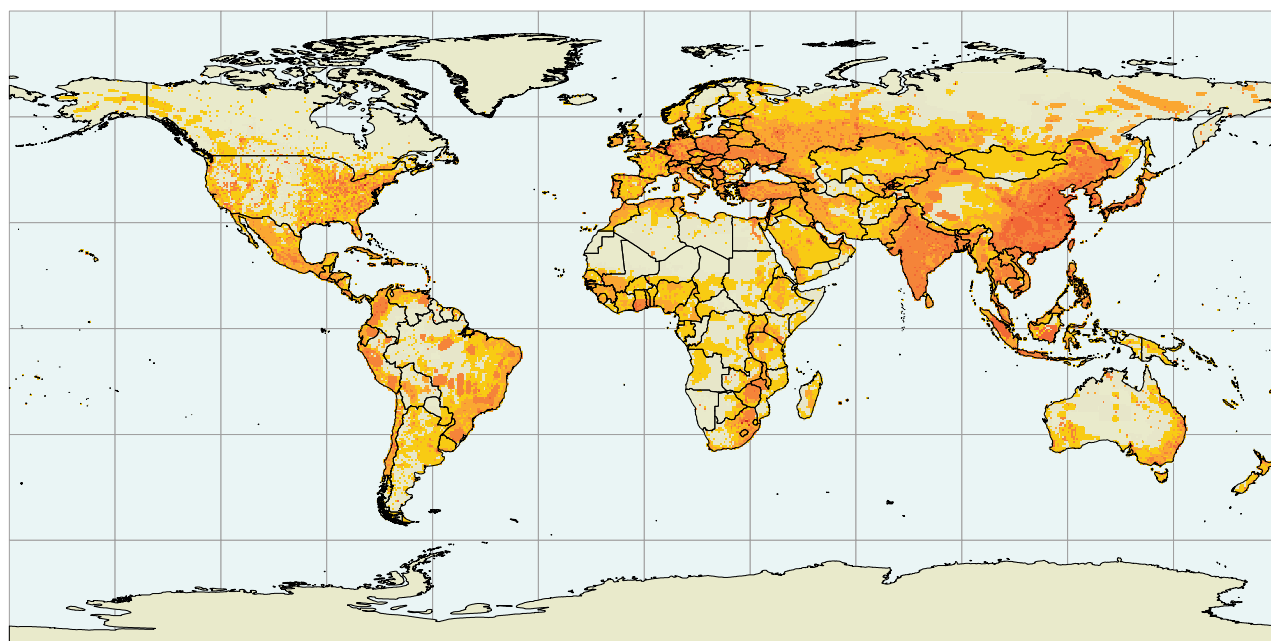


Figure 2.6. Global distribution of anthropogenic atmospheric emissions of mercury in 2005 to a 0.5° × 0.5° latitude/longitude grid. Source: AMAP/ UNEP (2008).

This re-analysis employed a common methodology, a more consistent information base for estimating certain emissions, and updating of the earlier inventories to account for improved knowledge gained during the past 15 years or so. The re-analysis also involved correcting certain questionable estimates in older inventories according to updated information on practices and technologies, including a few apparent errors. It also involved further revising the 2005 inventory for newly available data on regional Hg consumption that form the basis for estimates of emissions associated with ‘intentional-use’ sectors. The main results of this re-analysis are presented as follows.

Revised estimates of total emissions of Hg to air in 1990, 1995, 2000 and 2005 from ‘by-product’ and ‘intentional-use’ sectors are presented in Figure 2.7. ‘By-product’ sectors comprise: stationary combustion of fossil fuels in power plants and for residential heating; pig iron and steel production; non-ferrous metal production; cement production; industrial-use mercury production; large-scale gold production; and minor ‘other’ sources. Mercury emissions from the chlor-alkali industry are accounted in the ‘by-product’ sector inventory. Intentional-use sectors include artisanal and small-scale gold mining; emissions from cremation; secondary steel production; and waste disposal (including waste incineration). The data for emissions from ‘intentional-use’ sectors are regarded as conservative estimates.

Regional trends in combined emissions from ‘by-product’ and ‘intentional-use’ sectors for 1990, 1995, 2000 and 2005 are summarized in Figure 2.8.

Revision of the 1990, 1995 and 2000 inventories resulted in a significant reduction in total ‘by-product’ sector emission estimates compared to those previously published (Pacyna and Pacyna, 2002, 2005; Pacyna et al., 2006, AMAP/UNEP, 2008) estimates (see Table 2.2). Newly compiled information on consumption and use of Hg allowed new inventories for emissions from ‘intentional-use’ sectors to be prepared for 1990, 1995 and 2000. These changed the sectoral patterns, and

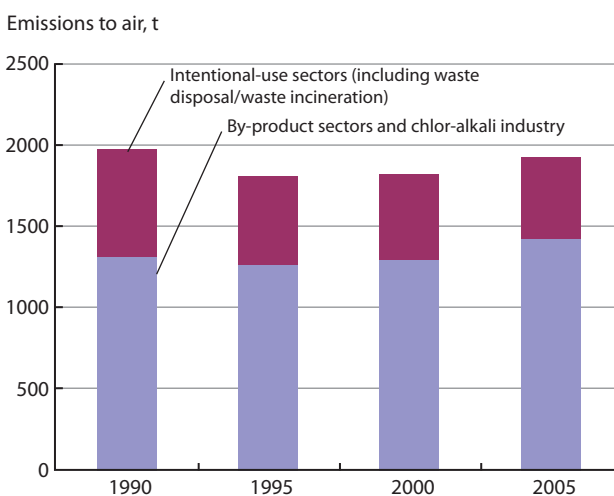


Figure 2.7. Revised estimates of total global anthropogenic mercury emissions to air from ‘by-product’ and ‘intentional-use’ emission sectors. Source: AMAP (2010); AMAP global mercury emission inventory v6.

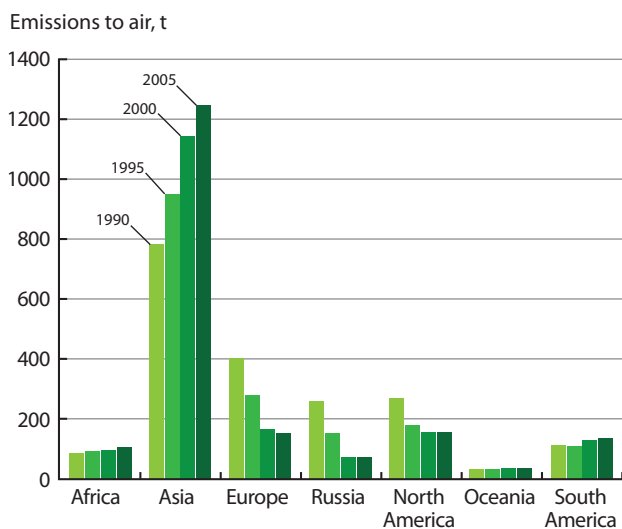


Figure 2.8. Revised estimates of annual anthropogenic mercury emissions to air from different continents/regions. Source: AMAP (2010).

to a lesser extent the magnitude of ‘intentional-use’ sector emissions in 2005.

The differences in the revised estimates for the emissions presented in Table 2.2 exceed the reported uncertainties associated with these estimates (which vary by about  $\pm 20$ -40% for the main industrial sectors, depending on the region). See AMAP (2010) for a detailed description of the revision of the historical emission inventories.

The newly constructed emissions inventories for 1990, 1995, 2000 and 2005 represent a more consistent set of global inventories of Hg emissions to air than those previously available, in terms of the underlying data and the methods used to produce and compile the estimates for various countries and source sectors. For the revised emissions inventories, the same emission factors (expressed as emissions of mercury per industrial activity unit) used in preparing the 2005 inventory (AMAP/UNEP, 2008) were applied to activity data (e.g. statistical information on coal consumption, metal production, cement production) from the corresponding year. The revised inventories have also been geospatially distributed (to a 0.5 by 0.5 degree latitude/longitude grid) using a consistent approach. In practice this required ignoring information on emissions from specific point sources and geospatially distributing all emissions according to a series of ‘surrogate’ data distributions that reflect the geospatial distributions for the sectors concerned. The ‘surrogate distributions’ used are those employed for the 2005 inventory as reported by AMAP/UNEP (2008).

Table 2.2. Differences between the originally-published global inventories of anthropogenic mercury emissions to air and the revised inventories for 1990, 1995, 2000 and 2005 (original inventories from Pacyna and Pacyna, 2002, 2005; Pacyna et al., 2006, AMAP/UNEP, 2008; revised inventories from AMAP, 2010).

	1990	1995	2000	2005 (v6)
Original total inventory	1732 <sup>a</sup>	2214 <sup>a</sup>	2190 <sup>a</sup>	1926 <sup>b</sup>
Revised total inventory	1967 <sup>b</sup>	1814 <sup>b</sup>	1819 <sup>b</sup>	1921 <sup>b</sup>
Difference	235	-400	-371	-5

<sup>a</sup>By-product sectors only (plus waste incineration for Europe (EU countries), USA and Canada); <sup>b</sup>by-product and intentional use sectors combined.

## 2.3. Are natural sources significant contributors of mercury to the Arctic environment?

### 2.3.1. Global natural emissions and re-emissions

Mercury occurs in the Earth’s crust, especially as the mineral cinnabar (Hg(II) sulfide: HgS). The metal is released naturally via weathering of rocks and as a result of volcanic/geothermal activities that constitute primary natural sources of Hg. According to Sunderland and Mason (2007), the pre-industrial world carried about 1600 tonnes of Hg in the atmosphere, 107 000 tonnes in the upper ocean, 194 000 tonnes in the deep ocean, and about 900 000 tonnes in surface soil. In addition to primary sources, deposited oxidized Hg may be reduced via photochemical or biological processes and re-emitted to the atmosphere. Re-emission of Hg occurs from soil and vegetation as well as from sea surfaces and is considered significant in comparison to primary emissions. As a consequence, the Hg concentration in the atmosphere is determined not only by primary sources (both natural and anthropogenic) but also to a significant degree by re-emission from environmental reservoirs.

These re-emission cycles were also active in the pre-industrial environment, re-cycling Hg released from natural sources. It is likely that, prior to the industrial period, Hg in the environment was more or less in a steady-state with mobilization rates from geological reservoirs balanced by removal through long-term burial (in soils and sediments), and the various reservoir compartments (atmosphere, soils, oceans) were in equilibrium. Significant anthropogenic emissions since the start of the industrial period have disturbed this balance and the major environmental reservoirs are no longer in equilibrium.

Evaluations of natural emissions of Hg have been carried out as part of studies of global Hg budgets and fluxes using global Hg models (Shia et al., 1999; Seigneur et al., 2001, 2004; Lamborg et al., 2002a; Mason and Sheu, 2002; Selin et al., 2007). Flux estimates based on field measurements exist but represent only very limited geographical areas and limited time scales.

Some recent environmental Hg fluxes from global Hg models are shown in Table 2.3. Mercury sources in Table 2.3 are categorized into total emissions from land and total oceanic emissions. The land and oceanic sources are further separated into primary natural emissions and re-emissions. Natural sources correspond to estimates of fluxes in the ‘pristine’ (i.e., pre-industrial) environment, while re-emissions also include increases in emissions from natural surfaces caused

Table 2.3. Environmental mercury fluxes estimated from global mercury models.

Hg Fluxes (kt/y)	Lamborg et al., 2002a	Mason and Sheu, 2002	Selin et al., 2007	Mason, 2009	Friedli et al., 2009a
Natural emissions from land	1.0	0.81	0.5		
Re-emissions from land		0.79	1.5		
<i>Emissions from biomass burning</i>					0.675
(A) Total emissions from land	1.0	1.6	2.0	1.85 <sup>a</sup>	
Natural emissions from ocean	0.4	1.3	0.4		
Re-emissions from ocean	0.4	1.3	2.4		
(B) Total oceanic emissions	0.8	2.6	2.8	2.6	
(C) Primary anthropogenic emissions	2.6	2.4	2.2		
Total sources (A+B+C)	4.4	6.6	7.0		
(D) Deposition to land	2.2	3.52			
(E) Deposition to ocean	2.0	3.08			
Total deposition (D+E)	4.2	6.6	7.0	6.4	
Net load to land	1.2	1.72			
Net load to ocean (burial in sediments)	1.2 (0.4)	0.68 (0.2)			
Total net load (land + ocean)	2.4	2.4	2.2		
Other parameters					
Mercury burden in the troposphere (kt)	5.22	5.00	5.36		
GEM lifetime (y)	1.3	0.76	0.79		

<sup>a</sup>Including Hg(0) emissions (0.2 kt/y) in response to AMDEs in polar regions. Biomass burning is not included in the emissions from land in this table.

by anthropogenic emissions at present and in the past. Primary anthropogenic emissions correspond to direct emissions from human activities. The model results in Table 2.3 are based on similar primary anthropogenic emission values, i.e., 2.2 to 2.6 kt Hg per year. This is close to that from the original global anthropogenic Hg emissions inventory for 2000 (2.2 kt/y; Pacyna et al., 2006). However, the estimates of total flux vary among the models, because of how re-emissions are treated by the different models. For example, unlike earlier models, Selin et al. (2007) predicted that the re-emission flux from the ocean was relatively high, even slightly greater than primary anthropogenic emissions.

The difference in estimates of re-emissions also reflects the importance of primary anthropogenic sources in comparison to total sources. In the Lamborg et al. (2002a) model, primary anthropogenic sources constitute about 60% of the total Hg emissions, whereas it is only 31% in the Selin et al. (2007) model. The net Hg load to land and ocean is defined in Table 2.3 as [total deposition] - [total emission from land and ocean]. The net load constitutes an annual loss of Hg from cycling, and in all estimates this loss is of the same magnitude as the total emissions from anthropogenic sources. In the Lamborg et al. (2002a) model, the Hg net load to the surface of the oceans is 1.2 kt/y. About 1.8 kt of the Hg in the ocean's surface layer is scavenged by particles each year and removed to the deeper layers of the ocean, but is compensated by 0.6 kt/y upwelling. Hence, the net load of Hg to oceanic surface water is estimated to be zero at present. In contrast, Hg is accumulated in the deep ocean at a rate of about 1.2 kt/y, of which 0.4 kt/y is buried in sediments of the sea floor. In the Mason and Sheu (2002) model, the ocean is treated in a somewhat more simplified manner. The load to the ocean is 0.68 kt/y, of which 0.2 kt is buried in sediments each year. With regard to the net Hg load to land, Mason and Sheu (2002) predicted a larger load than Lamborg et al. (2002a). Divalent Hg bonds strongly to thiol (SH<sup>-</sup>) groups in organic matter in soils, and is therefore to a large extent accumulated in the soil (Meili et al., 2003; Skjllberg, 2010).

One important aspect of the cycling of Hg in the environment is wildfires and biomass burning. Growing biomass and organic surface soils contain Hg originating from atmospheric deposition. When organic material is burned in accidental wildfires or intentional burning for forest clearance, the associated Hg is released back to the atmosphere. The global emission of Hg from this source category has been estimated at  $675 \pm 240$  t/y (Friedl et al., 2009). This is a significant contribution to the atmospheric pool of Hg and needs to be taken into account when calculating global mass balances of Hg for atmospheric modeling. The largest emissions occur in regions where boreal and tropical forests are burned, whereas burning of agricultural residues are assumed to contribute very little Hg. The uncertainty in this estimate is large due to incomplete information on the occurrence of fires, the Hg content of the organic material, and the degree to which the Hg is released during the fire.

From a policy perspective, this Hg emission should be treated partly as a re-emission driven by natural processes (i.e., wildfires), and partly as an emission under human control (intentional burning, forest clearance). Reducing the global intensity of forest clearance and biomass burning would thus have the additional beneficial effect of reducing the remobilization of Hg.

### 2.3.2. Natural contributions of mercury to the Arctic environment

Globally the residence times of Hg in the global upper ocean (~70 y in the pre-industrial period and ~27 y now; Sunderland and Mason, 2007) and in air (~0.7 y in both pre-industrial and present times) are long relative to the time taken for these media to transport into the Arctic (decades and weeks, respectively). For this reason, natural Hg has historically been and continues to be delivered to the Arctic from regions outside the Arctic both through the atmosphere and the ocean. Within the Arctic itself, the natural Hg cycle also continues through the release of

Hg by weathering, and the transfer of Hg from soils, sediments and vegetation into aquatic systems through volatilization, fires, dust and sediment resuspension. Therefore, the natural Hg cycle (Figure 2.9), as inferred from records in ancient material, is significant and provides a ubiquitous base concentration of Hg in all environmental media to which has been added the Hg released by human activities during the past two centuries.

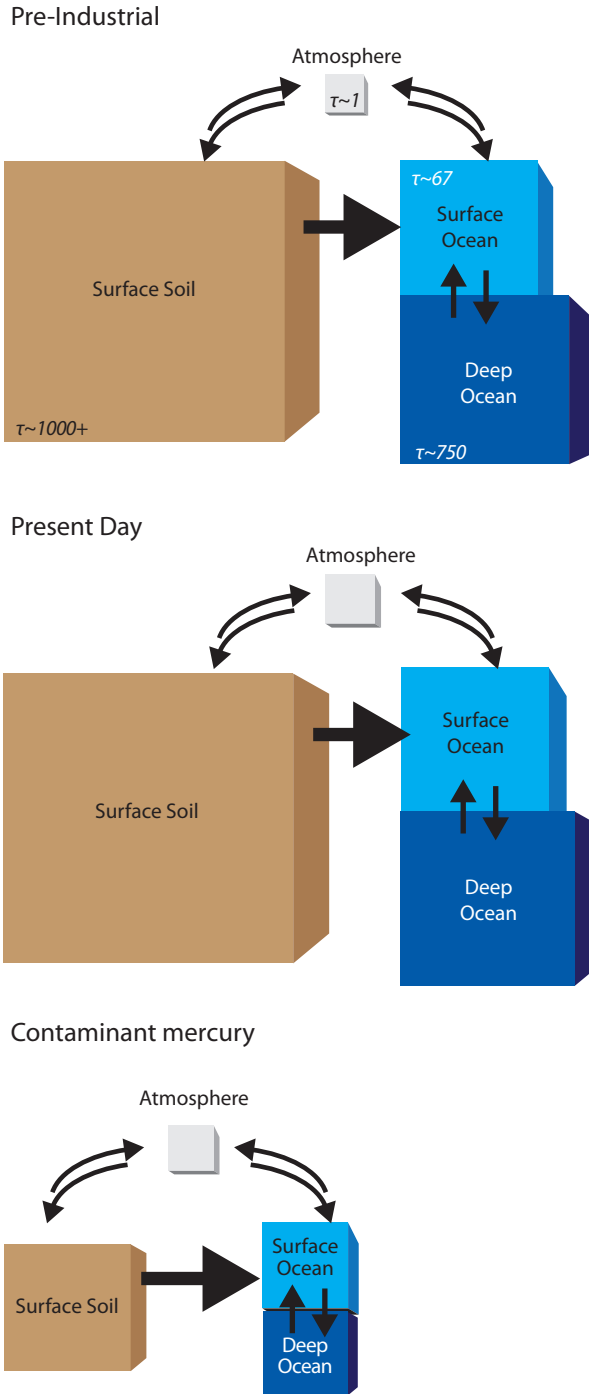


Figure 2.9. Major global mercury reservoirs and residence times in pre-industrial times. The sizes of the boxes reflect the relative amounts of mercury contained within each reservoir; values within boxes are average residence times in years. Adapted from Sunderland and Mason (2007).

### 2.4. What are the relative importance of and processes involved in atmospheric, oceanic, riverine and terrestrial inputs of mercury to the Arctic?

The Arctic Ocean and Hudson Bay are both semi-enclosed mediterranean seas, which provide the opportunity to calculate Hg budgets and therefore make direct comparisons of the relative importance of inputs to these systems (see Figure 2.10 and Figure 2.11). For Hudson Bay, Hare et al. (2008) also compared the modern Hg budget with one estimated for pre-industrial times. Detailed discussions of how the budget components were estimated and potential errors in the estimates are given in the respective publications. Briefly, the budgets depend upon reasonably well-balanced sediment and water budgets developed for both regions (Stein and Macdonald, 2004; Kuzyk et al., 2009). In the case of the Arctic Ocean, a modified version of the Global/Regional Atmospheric Heavy Metal (GRAHM; Dastoor and Larocque, 2004) model was used to arrive at an estimate of net atmospheric flux of Hg into the Arctic Ocean. The estimated fluxes for the various pathways are based on Hg concentrations and fluxes for media selected following comprehensive literature surveys (Table 2.4). For the Arctic Ocean as a whole (Figure 2.10), the largest single source of Hg was net atmospheric deposition, which contributed 48% (98 t/y) of the total annual Hg input (Outridge et al., 2008). The GRAHM model incorporates a re-emission term of 133 t/y and evasion of 12 t/y (thus, gross flux was 243 t/y). Of the net flux, 46% (45 t) occurred during springtime and 54% (53 t) during the rest of the year. Inflows from the Atlantic and Pacific Oceans (23%), and coastal erosion (23%) contributed most of the remaining total Hg to the system; rivers were collectively a minor source.

In contrast to the Arctic Ocean, for Hudson Bay, rivers were the largest single source (41%) followed in importance by the

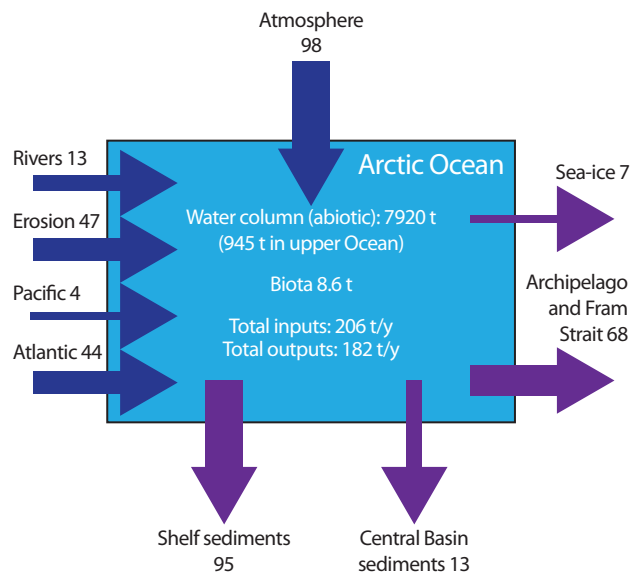


Figure 2.10. Mass balance model of total mercury in the Arctic Ocean with flux components estimated independently as described by Outridge et al. (2008). Flux units are t/y.

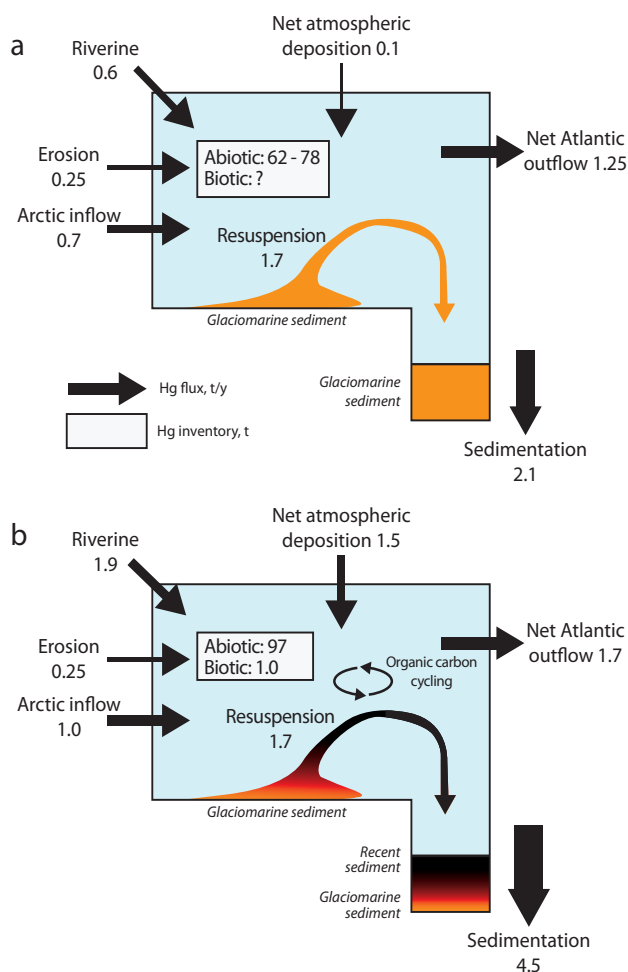


Figure 2.11. Mass balance model for total mercury in the Hudson Bay marine system; (a) for the pre-industrial period and (b) for the modern era. Source: Hare et al. (2008).

atmosphere (32%) and ocean inflow (22%) Hg fluxes (Hare et al., 2008). The difference between the Arctic Ocean and Hudson Bay can be partly attributed to the ‘edge effect’ of riverine inputs, which are relatively larger for smaller bodies of water. Another reason for differences between the two locations was that Hare et al. (2008) estimated the atmospheric deposition (1.5 t/y) from field measurements of atmospheric deposition, snowpack re-emission and seawater evasion, although the GRAHM model was used to set the maximum upper limit of 13.6 t/y.

The large difference between GRAHM model results and field measurements of atmospheric inputs in these budgets underscores what is widely regarded as the central uncertainty

in Arctic Hg science – What is the actual net deposition from the atmosphere that accumulates in the water? Modeled deposition estimates incorporating gross flux including AMDE effects range from 100 t/y for areas north of 70° N (Banic et al., 2003), to 325 t/y comprising 100 t/y from AMDEs and 225 t/y from other processes (Ariya et al., 2004). Other model results fall within these limits (208 t/y for ‘the Arctic’ (Skov et al., 2004); and about 150 to 300 t/y in polar spring only (Lindberg et al., 2002)). None of these studies allowed for post-AMDE re-emission or oceanic evasion, nor have they been validated by actual flux measurements.

For the Arctic Ocean, an independent estimate of net atmospheric input, based on field measurements of parameters associated with atmospheric flux, was calculated by Outridge et al. (2008) as,

net wet and dry deposition in winter/spring + wet and dry deposition during summer/autumn – evasion.

This approach, which employed data from direct measurements of wet deposition in the Arctic (Fitzgerald et al., 2005; Sanei et al., 2010), springtime snowmelt at many sites across the Arctic, and shipboard-based estimates of evasion from the ocean, produced a net atmospheric deposition to the Arctic Ocean of 8.4 t/y, over an order of magnitude lower than that provided by the GRAHM model. The net deposition rate (18.4 t/y), which was calculated without considering evasion, was similar to the 23 t/y calculated for the ‘High Arctic Ocean’ on the basis of snowpack sampling by Lu et al. (2001), and to the  $27 \pm 7$  t/y calculated from a net atmospheric flux of  $2.8 \pm 0.7 \mu\text{g}/\text{m}^2/\text{y}$  for lakes in northern Alaska (Fitzgerald et al., 2005). More work using a variety of methodological approaches is essential to resolve the uncertainty in the atmospheric contribution to Arctic ecosystems, especially as it will be this term that should be most immediately affected by emission controls.

For the terrestrial Arctic (land and lakes), almost all of the Hg input will occur from the atmosphere via wet and dry deposition. Near the coast, Hg deposited from the atmosphere may also include a component that has recently been recycled out of the ocean as Hg(0) or dimethylmercury (DMHg) (e.g., St. Louis et al., 2007; Hammerschmidt et al., 2007). Some of the Arctic’s drainage basins extend well beyond the Arctic Circle and, therefore, these southern drainage basins provide a source of Hg entering the Arctic as particulate or dissolved components in river flow. Mercury transported into the Arctic in this manner could include natural Hg as well as Hg from human activities within the southern drainage basins (e.g., mining, combustion), or Hg transported initially by the atmosphere and then deposited into these basins.

Table 2.4. Total mercury masses and the relative loadings from major input pathways into the Arctic Ocean and Hudson Bay: data from Outridge et al. (2008) and Hare et al. (2008), respectively. Mercury masses expressed as tonnes per year; relative loadings (in square brackets) are expressed as percentages of the total inputs. Hudson Bay data are for the modern era – see Figure 2.11b).

Pathway	Arctic Ocean	Hudson Bay
Ocean currents	48 [23%]	1.0 [22%]
Net atmosphere	98 [48%]	1.5 [32%]
Rivers	13 [6%]	1.9 [41%]
Coastal erosion	47 [23%]	0.25 [5%]
Total inputs (t/y)	206	4.65

Mercury input pathways to Arctic terrestrial ecosystems and lakes are poorly quantified. No work comparable to the oceanic mass studies has been done for Arctic terrestrial ecosystems, and only limited data are available for lakes. A Hg input and fate study by Fitzgerald et al. (2005) in a series of Alaskan lakes found that catchment soil erosion was the single most important total Hg input on average, followed by wet deposition and catchment runoff.

## 2.5. What is the influence of mercury speciation on total mercury transport by air?

### 2.5.1. Atmospheric transport and atmospheric chemistry – the status of present understanding

Mercury transported via the atmosphere can enter Arctic ecosystems following its deposition in aqueous, gas and particulate phases. Therefore the Hg species and mechanisms involved in transport through air, *in situ* chemical transformations, and the balance between deposition and re-emission at the surface, are important factors in the net atmospheric loading of Hg to the Arctic.

#### 2.5.1.1. Atmospheric mercury species

One of the most important properties of Hg regarding environmental concerns is its ability to exist as a gas in the atmosphere. Both anthropogenic and natural Hg emissions consist for the most part as Hg(0), i.e. gaseous elemental mercury (GEM), and in most circumstances approximately 98% of airborne Hg is GEM. The atmospheric residence time of Hg has been estimated at around 0.7 to 1.4 years (Schroeder and Munthe, 1998; Selin et al., 2007 and references therein), which is long enough for distribution on hemispherical scales before it is eventually oxidized and deposited to ground and water surfaces (Schroeder and Munthe, 1998). According to measurements, GEM is fairly uniformly distributed with concentrations of around 1.7 ng/m<sup>3</sup> in the Northern Hemisphere and 1.3 ng/m<sup>3</sup> in the Southern Hemisphere (Slemr et al., 2003). The higher values in the Northern Hemisphere are consistent with major industrial Hg sources being predominately located there. GEM is only to a small extent dry deposited to ground and vegetation or washed out by precipitation, but can be oxidized in the atmosphere forming divalent Hg species (Hg(II)) which are more easily removed from the atmosphere. Divalent Hg is found in both the gaseous and the particulate phase as well as in rainwater, however, the exact chemical compositions of these oxidation products are not yet known. The gaseous fraction of oxidized Hg is referred to as 'reactive gaseous mercury' (RGM) or 'gaseous oxidized mercury' (GOM). RGM is operationally defined as the fraction of gaseous Hg that can be sampled using a denuder measurement method (Landis et al., 2002; Steffen et al., 2008a), with species like HgCl<sub>2</sub>(g) and HgBr<sub>2</sub>(g) as likely candidates. The vapor pressures of Hg halides are relatively high, for example, P(HgCl<sub>2</sub>) = 0.017 Pa at 298 K (which corresponds to a saturation mixing ratio of 170 ppb). Due to the relatively high solubility of RGM, washout is an efficient

removal process yet it is more readily dry deposited on water surfaces and on vegetation than Hg(0). Total gaseous mercury (TGM) is another operationally defined Hg fraction. TGM includes GEM plus other possible gaseous Hg species, such as RGM, that may also be detected when measuring gaseous Hg by the commonly used gold-trap method.

Mercury is also found in aerosols originating from direct emissions or adsorption of atmospheric Hg onto already existing particles in the atmosphere. The abbreviation TPM (total particulate mercury) is used in the literature and it normally denotes the concentration of particulate Hg obtained with open face air filter samplers. Total particulate Hg means that the sampling is not made in a size fractionated manner. If Hg in the fine mode (< 2.5 µm particle size) is sampled it is sometimes denoted as fine particulate mercury (FPM) or simply referred to as particulate mercury PHg.

Dimethylmercury (CH<sub>3</sub>HgCH<sub>3</sub>) is formed in the oceans and its presence in the atmosphere is believed to be due to emission from ocean surfaces (Pongratz and Heumann, 1999). Sewage plants and landfills (among others) also emit DMHg, although these sources are of minor importance in comparison to the oceans and, as well, the emitted DMHg does not travel long distances in the atmosphere to the Arctic. Methylmercury (MMHg) compounds are found in rainwater and have also been detected in the gas phase (Munthe et al., 1993).

#### 2.5.1.2. Atmospheric transport

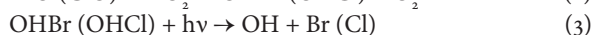
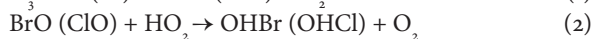
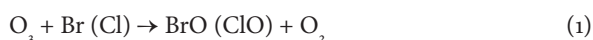
Mercury is transported to the Arctic from source regions mainly during the winter and spring seasons (Raatz, 1984) and this transport is influenced by atmospheric circulation patterns including the Pacific North American (PNA) and the North Atlantic Oscillations (NAO) (Wallace and Gutzler, 1981; Barnston and Livezey, 1987; Macdonald et al., 2005). Long-range atmospheric transport of Hg consists mainly of GEM, because of its relatively long airborne residence time of 0.7 to 1.4 years (Schroeder and Munthe, 1998; Selin et al., 2007 and references therein). Global transport of GEM has been investigated in various modeling studies (Mason and Sheu, 2002; Lamborg, et al., 2002b; Seigneur et al., 2004; Selin et al., 2007; Stohl et al. 2007; Strode et al., 2009) but has also been verified by direct measurements. Long-range transport of GEM and other pollutants from Europe to the European Arctic was measured during an Arctic smoke event at Ny-Ålesund (Stohl et al., 2007). In winter and spring, transport of anthropogenic GEM emissions from Europe leads to the highest observed GEM concentrations at Ny-Ålesund (Hirdman et al., 2009). Similarly, long-range transport from Asia has been measured at observatories on the US West Coast and by airplane measurements (Jaffe et al., 2005; Weiss-Penzias et al., 2007). The origin of the air masses was inferred by measuring Hg:CO ratios and calculation of back-trajectories. Evidence for long-range transport of Hg(0) from Asian sources has also been reported from Storm Peak Laboratory in the Rocky Mountains, 1500 km inland from the Pacific Ocean (Obriest et al., 2008; Fäin et al., 2009b). Due to the shorter atmospheric residence time of RGM and particulate Hg, they may not be transported between continents (Schroeder and Munthe, 1998). On the other hand, particulate Hg, presumably associated with fine soot particles, seems to be a sensitive indicator of transport on the regional scale (Wängberg et al., 2003).

### 2.5.1.3. Oxidation of elemental mercury and formation of reactive gaseous mercury

Exactly how RGM is formed in the atmosphere remains a key question that is crucial to the understanding of atmospheric Hg chemistry and how atmospheric Hg enters other environmental media. The reactive capacity of the atmosphere is linked to photolysis reactions forming certain reactive radical species such as OH, HO<sub>2</sub> and Br. The reaction rates of mercury with atmospheric radicals and other atmospheric constituents, have been determined in laboratory experiments. This information has enabled the construction of chemical-meteorological models for Hg. With the help of these models, important chemical and physical processes can be studied and verified by comparison with field measurements. Several atmospheric models including descriptions of Hg chemistry have also been developed (see Section 2.6). However, critical kinetic information on Hg(0) gas phase reactions is still lacking, partly because kinetic investigations on Hg are experimentally difficult to perform. Despite these problems, the reactivity between Hg(0) and several oxidants in the atmosphere has been investigated. These studies have included the gas phase reactions between Hg(0) and O<sub>3</sub>, OH, Cl, Br and NO<sub>3</sub> (Hall, 1995; Tokos et al., 1997; Sommar et al., 1999, 2001; Ariya et al., 2002; Bauer et al., 2003; Pal and Ariya, 2004a; Donohoue et al., 2005, 2006). The experimental results have also been reviewed recently (Simpson et al., 2007a; Ariya et al., 2008; Steffen et al., 2008a). In most of the studied reactions, no gaseous Hg-containing products were identified. The ability to identify products is, if not necessary, at least very helpful when trying to demonstrate a certain reaction. Some of the reaction rates obtained in early studies between Hg(0) and O<sub>3</sub>, OH, Br and Cl may have been overestimated as a result of experimental difficulties (Bauer et al., 2003; Calvert and Lindberg, 2005).

Field measurements in polar regions indicate very fast atmospheric processes during springtime allowing GEM to be transformed and removed from the lower layer of the atmosphere on the scale of hours or days. This phenomenon, termed mercury depletion events, was first reported by Schroeder et al. (1998). Subsequently, AMDEs were confirmed to occur throughout the Arctic, sub-Arctic and Antarctic coasts (Lindberg et al., 2001; Ebinghaus et al., 2002; Berg et al., 2003, 2008a; Poissant and Pilote, 2003; Steffen et al., 2005). Concurrent with decreasing GEM, increasing concentrations of RGM are observed as well as increasing particulate Hg (Lindberg et al., 2001). Mercury is thus rapidly oxidized in the air producing RGM, some of which is quickly deposited onto the ice and snow surface.

These findings stimulated an intensive search for possible chemical reactions that are fast enough to explain the observations. Halogen chemistry is important during polar springtime. Ozone may become almost completely depleted in the atmospheric boundary layer (Bottenheim et al., 1986; Oltmans and Komhyr, 1986) because of its reactions with Br and Cl radicals (Reaction 1). The halogen radicals are recycled according to Reactions 2 and 3, making the ozone destruction very efficient (Barrie et al., 1988).



Recent Arctic and Antarctic field measurements showed an almost perfect match between removal of ozone and GEM (Schroeder et al., 1998; Lindberg et al., 2002; Temme et al., 2003; Gauchard et al., 2005; Sommar et al., 2007). Therefore, it has been suggested that Hg(0) also may react with halogen radicals (Simpson et al., 2007a and references therein; Steffen et al., 2009 and references therein). According to theoretical studies (Khalizov et al., 2003; Goodsite et al., 2004; Shepler et al., 2007), the Hg(0) + Br reaction may constitute an initial step in a chemical process leading to stable divalent oxidized Hg compounds. An excited intermediate, HgBr\*, is initially predicted (Reaction 4). The HgBr molecule may decompose through Reaction 6 and 7 or further react according to Reaction 8 to form a stable gaseous Hg(II) compound.



Whether this path is significant depends critically on the stability of the intermediate HgBr radical. Reactions 4 and 5 have been recently verified experimentally by Donohoue et al. (2006), with the rate coefficient shown in equation (I) below. The stated accuracy of equation (I) was  $\pm 50\%$  (Donohoue et al., 2006).

$$k_{4,5} (243\text{-}293 \text{ K}) = (1.46 \pm 0.34) \cdot 10^{-32} (T/298)^{-(1.86 \pm 1.49)} \text{ cm}^6 \text{ molecule}^{-2} \text{ s}^{-1} \quad (I)$$

The rate of Reaction 4-5 is  $3.8 \times 10^{-13} \text{ cm}^3 \text{ molecules per second}$  at 293 K and atmospheric pressure. As yet, no experimental results have been reported on Reactions 7 and 8 which describe the fate of the intermediate HgBr. However, assuming peak concentrations of bromine atoms of  $10^7$  to  $10^8 \text{ atoms/cm}^3$  under Arctic conditions, Donohoue et al. (2006) estimated the Hg(0) lifetime with respect to Reaction 4-5 to be in the range of 6 hours to 2.5 days, which is consistent with observations. Reactions 4 and 5 may also be important at much lower Br concentrations. Assuming an average concentration of Br radicals in the free troposphere of  $1 \times 10^5 \text{ molecules/cm}^3$ , the lifetime of Hg(0) is then estimated to be about 220 days. According to theoretical studies, HgBr may form stable RGM compounds according to Reaction 8 (Goodsite et al., 2004; Shepler et al., 2007). Recent observations of elevated RGM concentrations in the free troposphere also support the idea that RGM formation through halogen radical reactions could be important (Swartzendruber et al., 2006; Faïn et al., 2009a). High concentrations of RGM were frequently observed in dry tropospheric air originating from the northern Pacific Ocean (Faïn et al., 2009a). Air masses containing elevated RGM were found to be low in CO and other anthropogenic air pollution tracers. It was thus concluded that RGM was formed *in situ* via photolytically-induced reactions in the free troposphere (Swartzendruber et al., 2006; Faïn et al., 2009a).

Bromine atoms can be produced from a number of sources: one is sea spray and is thus connected to the marine boundary layer; a second source during polar spring is refreezing leads (open water areas in sea ice or between sea ice and the shore in which are found bromine-enriched brine and frost flowers). Here, Br<sub>2</sub> is released from bromide-enriched sea-ice surfaces. A



### 2.5.2.2. Observations of deposition

Mercury can be deposited onto snow surfaces through both wet and dry deposition processes. Dry deposition in coastal polar regions mainly corresponds to RGM formed during AMDEs (Lu et al., 2001; Lindberg et al., 2002; Ariya et al., 2004). However, the consequences of AMDE Hg deposition for Hg levels in the environment are still unclear. Brooks et al. (2006) published a mass balance for Hg at Barrow, Alaska, showing a net surface gain during a two-week AMDE period. Overall, the rate of deposition of Hg onto the snow is greater in Arctic coastal areas than in more southerly locations and inland areas (Lindberg et al., 2002; Douglas et al., 2005). The GRAHM model indicates springtime net deposition (both AMDE and non-AMDE processes) to the Arctic Ocean was about 45% of total (wet + dry) annual deposition (Outridge et al., 2008).

Mercury in surface snow following AMDEs is mainly found in its oxidized form (Hg(II)), with concentrations that can range from a few up to hundreds of ng/L (Lu et al., 2001; Lalonde et al., 2002; Lindberg et al., 2002; Steffen et al., 2002; Berg et al., 2003; Ferrari et al., 2004, 2005; Douglas et al., 2005; Lahoutifard et al., 2006; Steen et al., 2009, 2010). However, it has also been observed that, within a few days after each AMDE, about 80% on average of the deposited Hg in surface

snow is re-emitted as GEM back to the atmosphere (see Section 2.6.2). It is important to point out that these results are based on the snowpack concentrations of total Hg, rather than on mass balance studies of the atmospheric concentration of GEM. In Svalbard, Ferrari et al. (2005) reported that during seven AMDEs no increase in the concentration of Hg in the surface snow was observed. The authors suggested that the origin of the air mass prevailing at the time of the AMDE may play a significant role in the amount of Hg deposition observed. Douglas et al. (2008) reported elevated concentrations in the surface snow following AMDEs, and suggested that the crystal structure of the surface hoar frost, diamond dust and frost flowers was important in determining the rate of Hg deposition and accumulation in snow from AMDEs. Thus, deposition of Hg onto the snow surfaces in the Arctic, as a result of AMDEs, is not spatially homogeneous and the factors affecting such deposition must be well understood to address the impacts of AMDEs on Hg levels in the Arctic environment. The possible impact of AMDEs on Hg bioavailability has also not been adequately addressed. At Barrow, Scott (2001) reported a post-polar sunrise increase in bioavailable Hg in surface snow and an increasing ratio of bioavailable Hg to THg as the springtime progressed to annual snowmelt.

In terms of the atmospheric contribution to Hg in the Arctic,

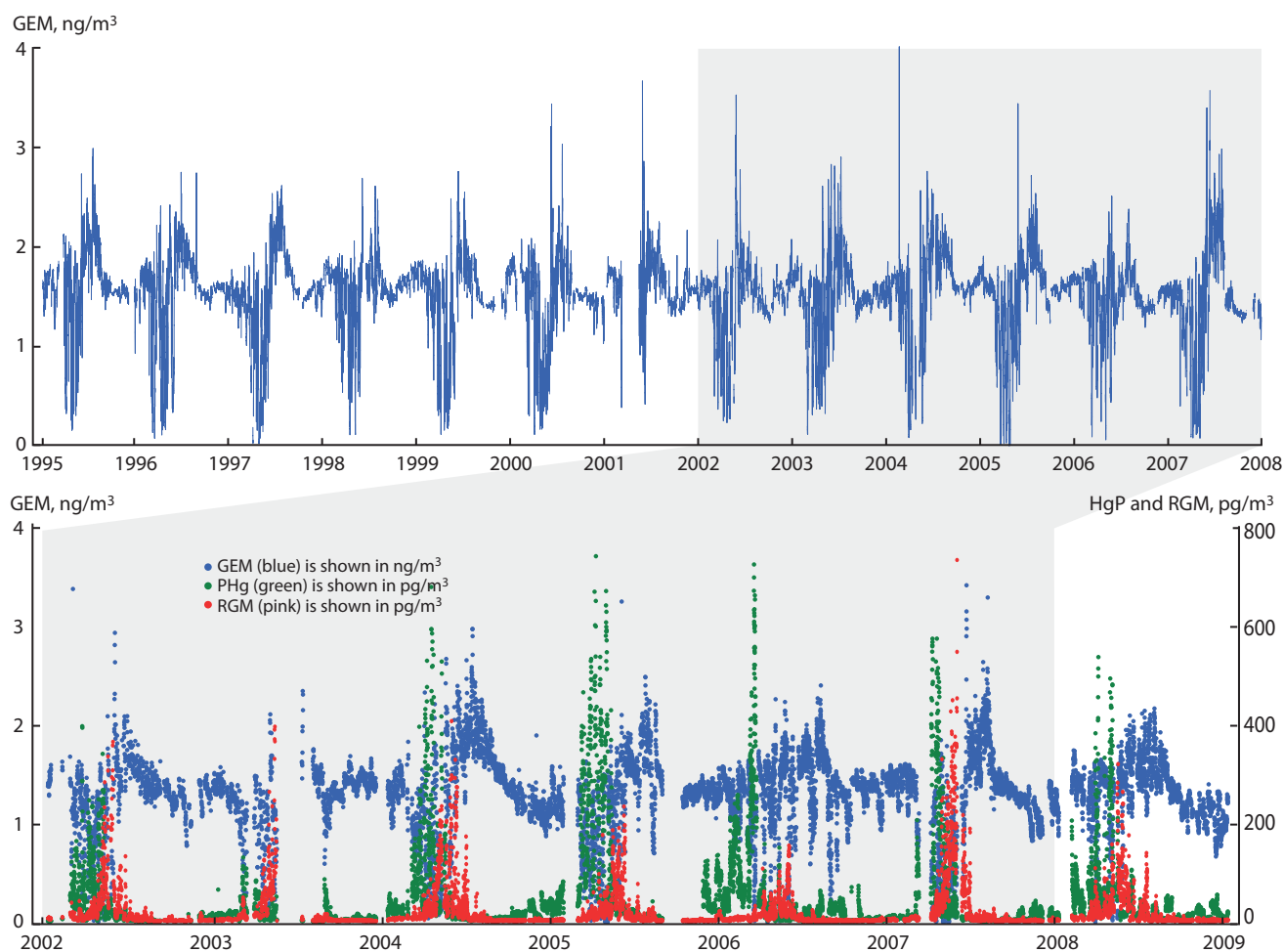


Figure 2.13. Time series for gaseous elemental mercury (six-hourly averaged data) concentrations at Alert, Nunavut, Canada from 1995 to 2008 (top) and time series of reactive gaseous mercury, particulate phase mercury and gaseous elemental mercury (three-hourly averaged data) concentrations from Alert 2002 to 2008 (bottom). Source: Alexandra Steffen, Environment Canada, pers. comm.

the largest limitation remains the paucity of knowledge of Hg speciation, and the net deposition rates of Hg. During a meeting of experts in 2003, the re-emission proportion of Hg from the surface after deposition from AMDEs, or release to other compartments, was identified as an essential missing component before true mass balance estimates could be made (Schroeder et al. 2003). Subsequently, an experts meeting in 2006 (Air Ice Chemical Interactions – AICI) determined that despite intense trans-Arctic springtime field campaigns this issue remained to be resolved. Model estimates of the atmospheric input to the Arctic region are discussed in Section 2.6.1.1. An updated summary of the snowpack-based literature concerning Hg re-emission after AMDEs is presented in Section 2.6.2.

### 2.5.3. Long term trends in gaseous elemental mercury

Worldwide atmospheric measurements up to the early 2000s suggested that GEM concentrations increased from the late 1970s to a peak in the 1980s and decreased to a plateau around 1996 to 2001 (Slemr et al., 2003). Data used in the reconstruction of the worldwide trend were collected at six sites in the Northern Hemisphere, two sites in the Southern Hemisphere and eight ship cruises over the Atlantic Ocean. More recently, a reconstruction of GEM levels in the air over Greenland Summit based on glacial firn sampling indicated that GEM increased from the 1940s to about the 1970s, decreased until the mid-1990s and has been stable since then (Faïn et al., 2009b).

Long-term datasets with at least five years of continuous instrumented measurements of atmospheric Hg concentrations are rare in polar regions. However, data have been consistently collected for at least five years from Alert, Canada (1995 to 2009 with automated monitors); Ny-Ålesund, Svalbard (1994 to 1999 with manual samplers, and 2000 to 2009 with automated monitors), and Amderma, Russia (2001 to 2002, and 2005 to 2009 with automated monitors). There are also multi-year datasets from Barrow, Alaska, and Station Nord, Greenland, however, they are not continuous or long-term.

To investigate annual trends in polar regions, it is important to take into account the strong seasonal variation caused by springtime decreases in GEM related to AMDEs, and summertime elevations in GEM levels caused by the re-emission of Hg deposited onto snow as well as evasion from oceans, freshwaters and the ground itself (see Chapter 3). These seasonal variations are much larger than any interannual changes and therefore it is challenging to discern statistically significant annual trends. A seasonal trends analysis of Alert data was undertaken and a statistically significant decrease was reported in the summer GEM concentrations (June – August) between 1995 and 2002 (Steffen et al., 2005). Temme et al. (2007) analyzed the same annual dataset, using a seasonal decomposition technique (in which annual trends are tested by sequentially removing seasonal data), and found the same summer declining trend up to 2002. However, no significant change for the overall period between 1995 and 2005 was found. Berg et al. (2004) reported no trends for GEM concentration at Ny-Ålesund for the period 1994 to 2002. When an extended time-series (1994 to 2005) was considered, Berg et al. (2008a) again reported no significant

trend at Ny-Ålesund. In both studies from Ny-Ålesund, the manually collected data were included for 1994 to 1999. In the first study, annual averages were used, whereas in the second study the trends were analyzed on winter, spring, summer and autumn means. More recently, a small, but statistically significant decreasing trend (-0.6% per year) has been reported in the mean annual concentration of GEM at Alert for the 13 years between 1995 and 2007 (Cole and Steffen, 2010).

There could be several reasons for the reported weak or insignificant trends in Arctic atmospheric Hg. Most of the available time-series cover the period from 1995 to 2005 during which total global anthropogenic emissions of Hg have not changed markedly (see Section 2.2.2), although there have been significant changes in emissions from particular source regions during this period. Mercury emissions from East Asia increased by 50% from 1990 to 2005 whereas emissions from Europe and North America have declined over the same period, resulting in smaller emissions trends overall compared to the 1970s and 1980s. These small net changes in background GEM concentrations also may be masked by seasonal and interannual variability, particularly at sites with shorter records. In addition, changes in the major atmospheric circulation patterns (Kahl et al., 1999) may complicate the relationship between changes in emissions and trends in Arctic atmospheric GEM.

Other long-term atmospheric Hg trend studies based on Arctic observations include that of Li et al. (2009), who reported a decrease of 3% per year in airborne filterable (i.e. particulate) Hg in summer and autumn samples collected between 1974 and 2000 at Resolute, Canada. A similar decline in GEM concentrations after about 1970 was reported from a Greenland Summit firn core by Faïn et al. (2009b). This declining trend largely predates the start of instrumented gas phase Hg monitoring in the Arctic. The reported declines at Summit and Resolute may reflect the significant decreases in anthropogenic emissions of Hg between the 1970s and 1990s and possibly (in the case of Li et al., 2009) reductions in the proportion of particulate Hg resulting from the global introduction of control technology to remove particulates from industrial plant emissions (see Section 2.2.2).

Studies using sediment and peat cores have been used to estimate trends in depositional fluxes of Hg (see Section 2.7). However, trends based on direct measurements of Hg in wet and/or dry deposition are unavailable for most Arctic areas. Except for the recently initiated Kodiak station in Alaska, the Mercury Deposition Network (MDN) in North America does not include Arctic or sub-Arctic sites. At several Northern European stations, a comparison of wet deposition fluxes for the periods 1995-1998 with 1999-2002 showed an overall decrease of 10-30%, which was attributed to reduced emissions in industrial areas of Europe (Wängberg et al., 2007). A recent evaluation of deposition fluxes during three time periods (1995-1998, 1999-2002, 2003-2006) and also including the Pallas station (located in Finland above the Arctic Circle) indicated no significant trends in TGM or deposition at Pallas. However, a continued decrease in Hg deposition was found at most Northern European stations while trends in TGM were variable or insignificant (Wängberg et al., 2010).

As part of the present Assessment, statistical reanalyses of GEM data from all Arctic stations have been carried out using a consistent methodology. Figure 2.14 shows the time

trends of median concentrations of GEM at the three long-term High Arctic monitoring sites for the autumn period (October to December). This period was selected because background GEM levels are least affected by fluctuations due to AMDEs and re-emissions of deposited Hg. The figure presents automated monitoring data only from Alert (1995 to 2008), Ny-Ålesund (2000 to 2009) and Amderma (2001 to 2002, 2005 to 2008) indicating the period of overlap of data from 2000 to 2008. Statistical runs were performed on these data sets using the PIA statistical application (Section 5.3.3.2). Runs were performed separately for each month using monthly (median) index values and also run for a combined October to December period.

Results from the October to December datasets did not reveal any statistically significant trends, although, a significant decreasing trend (-0.67% per year;  $p < 0.05$ ) was observed at Alert when considering data for the month of September alone. The time series indicated non-significant decreasing trends during autumn of about -0.6% per year at Alert (1995

to 2008) and -1% per year at Amderma (2001 to 2008), but an increasing trend (+1.5% per year) at Ny-Ålesund (2000 to 2009). The results from Alert are in keeping with those reported by Cole and Steffen (2010) on the annual data, indicating that the autumn period may be a good proxy for the annual trends. The results from Amderma should be interpreted with caution, since the site location changed in 2004; considering only the data since 2005 shows an increasing trend.

Clearly, many challenges exist in trying to ascertain long-term trends in GEM in the Arctic region. However, the availability of increasingly long-term time series, and the use of Hg samples archived in glacial ice or on particulate filters collected over the past few decades, has provided opportunities to elaborate trends that did not previously exist. Significant atmospheric processes affect GEM levels in polar regions, and further collection of data is required in the Arctic to truly discern long-term trends over the entire region.

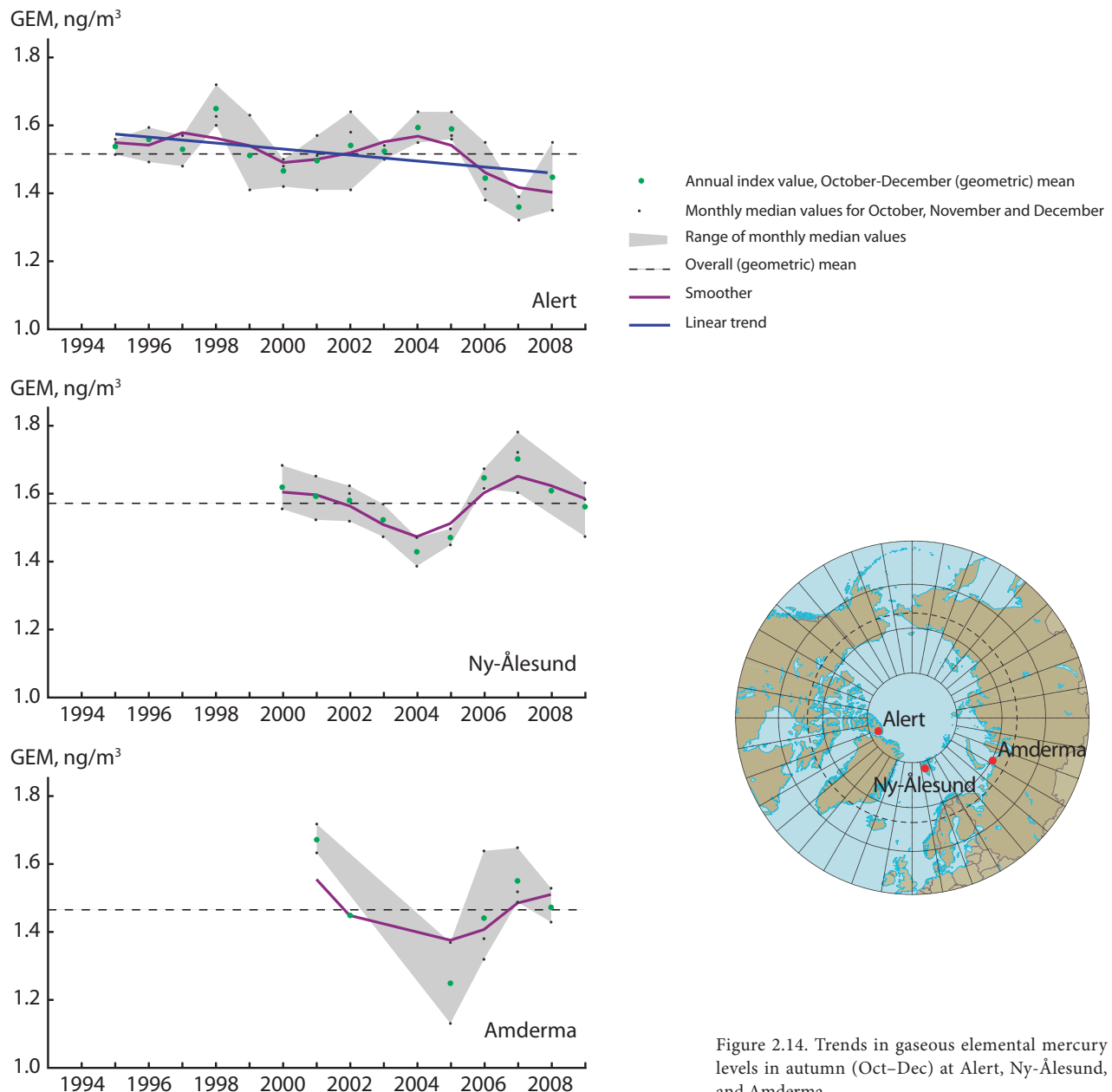


Figure 2.14. Trends in gaseous elemental mercury levels in autumn (Oct-Dec) at Alert, Ny-Ålesund, and Amderma.

## 2.6. What is known about the net atmospheric mass contribution of mercury to the Arctic?

### 2.6.1. Modeling atmospheric mercury transport to the Arctic

#### 2.6.1.1. Net deposition results from atmospheric modeling

In recent years, atmospheric chemical models have become powerful tools in assessing and understanding the level of contaminants in the environment, given the limited coverage of existing monitoring networks. Mercury models are employed to estimate Hg ambient concentrations and deposition, to estimate source attribution, explain long-term trends and to predict future levels of pollution. The models complement direct measurements by providing spatial coverage and detailed information on Hg budgets in the Arctic environment.

Atmospheric Hg models attempt to represent cycling of Hg in the atmosphere starting from Hg emissions to the air, including contemporary anthropogenic emissions, natural emissions, and re-emissions of Hg of both anthropogenic and natural origin, to its subsequent deposition to terrestrial and aquatic surfaces. Modeling atmospheric Hg requires extensive treatment of multiple Hg species (i.e. GEM, RGM and particulate Hg) that exhibit different properties and exist in multiple phases of the atmosphere. Main Hg processes implemented in the models are gas and aqueous phase chemistry, exchange processes in and below clouds, wet and dry deposition, boundary layer and cumulus cloud mixing and transport.

Owing to the global scale of Hg transport, hemispheric or global-scale atmospheric models are employed to estimate the atmospheric Hg mass contribution to the Arctic. Current Hg models are primarily constrained by measurements of surface air concentrations of GEM and wet deposition fluxes in North America and Europe, due to the lack of global measurements. Models also utilize a small number of available measurement data of RGM and particulate Hg ambient concentrations, vertical

Table 2.5. Characteristics of the participating atmospheric mercury models.

Model	GRAHM (v1.2)	GLEMOS (v1.0)	GEOS-Chem (v8.2)	DEHM (v5.1)
Domain	Global	Global	Global	Hemisphere
Spatial resolution				
Horizontal	1° × 1°	5° × 5°	4° × 5°	150 × 150 km
Vertical	28 levels; top 10 hpa			
Emission				
Anthropogenic, t/y	1925	1925	1925	1469 <sup>a</sup>
Natural and re-emission, t/y	3500 <sup>b</sup>	4230 <sup>b</sup>	6235-6770 <sup>c</sup>	Inflow from boundaries
Gaseous chemistry				
Oxidation agents	O <sub>3</sub>	O <sub>3</sub> , OH, Cl <sub>2</sub>	Br	O <sub>3</sub>
Oxidation rates <sup>d</sup>	O <sub>3</sub> : 3 × 10 <sup>-20e</sup>	O <sub>3</sub> : 3 × 10 <sup>-20e</sup> OH: 8.7 × 10 <sup>-14e</sup>	8.1 × 10 <sup>-14e,f</sup>	O <sub>3</sub> : 3 × 10 <sup>-20e</sup>
RGM/HgP partitioning	O <sub>30</sub> Oxidation product-1:1	O <sub>3</sub> oxidation-HgP OH oxidation-HgP Cl <sub>2</sub> oxidation-RGM	Br Oxidation – 1:1 RGM adsorption to sea-salt aerosols parameterization	O <sub>3</sub> Oxidation product-1:1; RGM adsorption to black carbon
Reduction agents	none	none	none	none
Aqueous chemistry				
Oxidation agents	O <sub>3</sub> , OH, HOCl/OCl <sup>-</sup>	O <sub>3</sub> , OH, HOCl/OCl <sup>-</sup>	none	O <sub>3</sub> , OH, HOCl/OCl <sup>-</sup>
Reduction agents	hv, SO <sub>3</sub> <sup>=</sup>	SO <sub>3</sub> <sup>=</sup>	hv	SO <sub>3</sub> <sup>=</sup>
AMDE	yes	yes	yes	yes
Chemistry <sup>g</sup>	over sea ice: Br, BrO, Cl, Cl <sub>2</sub> , O <sub>3</sub>	Br, BrO, Cl <sub>2</sub> , O <sub>3</sub>	over sea ice: Br	First order oxidation Over sea ice
RGM/HgP partitioning of Br oxidation	RGM	RGM	1:1	
Br oxidation rate <sup>h</sup>	3.2 × 10 <sup>-12e</sup>	1.1 × 10 <sup>-12e</sup>	8.1 × 10 <sup>-14e,f</sup>	
Br concentrations in Arctic boundary layer	From satellite data derived BrO conc.	From Satellite data derived BrO conc.	From fixed BrO conc.	Parameterization based on sea ice and temperature
Re-emission from snow	yes	no	yes	No
Wet deposition				
In-cloud	RGM(rain/snow), HgP(rain/snow)	RGM(rain/snow), HgP(rain/snow)	RGM(rain), HgP(rain)	RGM(rain/snow), HgP(rain/snow)
Below-cloud	RGM(rain/snow), HgP(rain/snow)	RGM(rain/snow), HgP(rain/snow)	RGM(rain), HgP(rain/ snow)	RGM(rain/snow), HgP(rain/snow)
Precipitation rates	Model predicted	Model predicted	Model predicted	Model predicted
Dry deposition	Hg(0), RGM, HgP	Hg(0), RGM, HgP	Hg(0), RGM, HgP	RGM, HgP
Source	Dastoor et al., 2008	Travnikov et al., 2009	Holmes et al., 2010	Christensen et al., 2004

<sup>a</sup> Total value for the hemispheric model domain; <sup>b</sup> prescribed fluxes globally with dynamic seasonal and diurnal variation; <sup>c</sup> dynamic fluxes from oceans and terrestrial biosphere; <sup>d</sup> only major oxidant rates shown; <sup>e</sup> temperature and pressure dependence applied; <sup>f</sup> rate at 0.1 ppt Br, 1 × 10<sup>6</sup> cm<sup>3</sup> OH; <sup>g</sup> gas phase chemistry in the polar boundary layer; <sup>h</sup> units: cm<sup>3</sup> molecule per second; rate at 298 K; 1 atm.

Table 2.6. Summary of atmospheric deposition estimates in the Arctic region.

Study location	Type of study	Gross or net deposition? <sup>a</sup>	Deposition, t/y	Model	Emissions inventory year	Source
Northern waters Arctic (north of Arctic Circle)	Atmospheric		50			Lu et al., 2001
Arctic Ocean	Atmospheric/model	Gross	208			Skov et al., 2004
	Model	Net	98	GRAHM v1.1		Outridge et al., 2008
	Field measurement (lit. review)		8.4			
North of 66.5° N	Atmospheric /model	Net	174 (range 150-181)	GRAHM v1.1	2005 v5	Dastoor et al., 2008
Barrow, Alaska	Atmospheric		100-300 (spring only)			Lindberg et al., 2002
North of 70° N	Atmospheric		100			Banic et al., 2003
North of 60° N	Atmospheric/model	Gross	325 (100 spring only)	GRAHM v1.0	2000	Ariya et al., 2004
North of 66.5° N	Atmospheric/model intercomparison study	Gross/net	131	GLEMOS v1.0	2005v5	Travnikov et al., 2009; this report
North of 66.5° N	Atmospheric/model intercomparison study	Net	143	GRAHM v1.2	2005v5	Dastoor et al., 2008; this report
North of 66.5° N	Atmospheric/model intercomparison study	Net	80	GEOS-Chem v8.2	2005v5	Holmes et al., 2010; this report
North of 66.5° N	Atmospheric/model intercomparison study	Gross/net	110	DEHM v5.1	2005v5	Christensen et al., 2004; this report

<sup>a</sup> Net: deposition estimate from model that includes fast re-emissions from snow; Gross: deposition estimate from model that does not account for (fast) re-emissions from snow; Gross/net: gross deposition estimates from models that are constrained such that these estimates are comparable to net deposition estimates.

profiles of GEM and fluxes of Hg from terrestrial and oceanic surfaces. Mercury modeling in the Arctic is further complicated by the very dynamic exchange of GEM between air and snow because of AMDEs (see Section 2.5). Photochemical oxidation of GEM by halogens, speciation of products, deposition pathways and re-volatilization of GEM from snow must be parameterized to estimate the net accumulation of Hg in the Arctic. Using a Hg model that includes these processes, Durnford et al. (2010) showed consistent reproduction of the AMDE cycles at six Arctic air measurement sites. Their results indicate that the GEM transformations are generally governed by very similar processes throughout the Arctic, involving bromine photochemistry in air and re-emission mediated by solar insolation on surface snow.

A number of models are currently making use of the 2005 (v5) spatially distributed anthropogenic emissions inventory developed by AMAP (AMAP/UNEP, 2008, see Section 2.2.2). Published model results (Skov et al., 2004; Ariya et al. 2005; Travnikov, 2005; Dastoor and Larocque, 2004, 2008; Durnford et al., 2010) have utilized earlier versions of the global emission inventories, for example, the 2000 inventory (Pacyna et al., 2006; Wilson et al., 2006) that did not include the full range of source sectors included in the 2005 inventory. As part of the current AMAP assessment, models have now also been run using the consistent series of historical emissions inventories (1990 to 2005) discussed in Section 2.2.2.

Four atmospheric Hg models incorporating springtime AMDEs in the Arctic have been developed to date (DEHM: Christensen et al., 2004; GLEMOS: Travnikov et al., 2009; GEOS-Chem: Holmes et al., 2010; GRAHM: Dastoor et al., 2008). The main differences between the recent versions of these models are summarized in Table 2.5, with the largest differences in natural emissions and re-emissions. An important difference between model specification of natural and re-emission (not shown here) is that, due to a lack of knowledge, different

approaches are used to distribute these emissions spatially. Other main differences are the major oxidants of GEM and the speciation of the reaction products included in the models. In the Arctic, the major differences are found in the GEM-Br oxidation rates, Br concentrations and spatial distribution and parameterization of re-emission of GEM from snow. Most recent versions of the four models were employed to estimate the Arctic Hg deposition and source attribution for 2005 using AMAP 2005 v5 anthropogenic emissions for this report.

The range of estimates of Arctic Hg deposition from the four model simulations performed for this Assessment, as well as previously published estimates and estimates from field measurements, are summarized in Table 2.6. The table distinguishes whether the estimates concern gross or net deposition (the latter including a re-emission term), and covers a variety of different models and emission inventories, which together account for the differences in the final estimates. Using DEHM, Skov et al. (2004) estimated a deposition of 208 t/y of Hg to the Arctic area north of the polar circle (66° 33' 38" N), of which 120 t/y was attributed to AMDEs. Ariya et al. (2004) estimated that 325 t/y of Hg is deposited in the Arctic north of 60° N, including 100 t/y deposited as a result of AMDEs using an early version of GRAHM that did not incorporate post-AMDE re-emission. Dastoor et al. (2008) incorporated bi-directional exchange of Hg fluxes in the Arctic in GRAHM to account for the fast re-emission of Hg from snowpack following AMDEs. They estimated 174 t/y net accumulation of Hg in snow with an uncertainty range of 150 to 181 t/y for the region north of 66.5° N. Brooks et al. (2006) measured Hg deposition, re-emission and net surface gain fluxes of Hg at Barrow, Alaska during an intensive measurement campaign for a two week period in spring (March 25 to April 7, 2003) as 1.7 µg/m<sup>2</sup>, 1.0 ± 0.2 µg/m<sup>2</sup> and 0.7 ± 0.2 µg/m<sup>2</sup>, respectively. Dastoor et al. (2008) found excellent agreement between model-derived fluxes at Barrow

( $1.8 \mu\text{g}/\text{m}^2$  deposition,  $1.0 \mu\text{g}/\text{m}^2$  re-emission, and  $0.8 \mu\text{g}/\text{m}^2$  net surface gain of Hg) and the above study. The most recent modeling estimates are shown in the last four rows in Table 2.6. Although GLEMOS and DEHM do not model the re-emission of Hg from snow explicitly, the average ambient Hg concentration of GEM in these models is constrained by measurements. Their deposition estimates, therefore, could be considered net flux in some sense. The net deposition estimates from the recent simulations of GRAHM, GLEMOS, GEOS-Chem and DEHM range between 80 to 143 t/y for the Arctic north of  $66.5^\circ \text{N}$ .

The spatial distributions of net deposition of Hg (gross deposition for GEOS-Chem) simulated by the four models are presented in Figure 2.15. The impact of model resolution is evident

in the simulation by GRAHM, which shows higher variability in deposition. All models, in general, portray an increasing north-to-south gradient in deposition that could be attributed to a coincident gradient in Br concentrations, proximity to emission sources and precipitation amounts. However, there are considerable differences between the deposition distributions within the Arctic and these mainly arise due to different approaches used in the models for Br activation in the Arctic boundary layer (Table 2.6). Large uncertainties associated with the production mechanism and concentrations of Br in the Arctic boundary layer, and an order of magnitude difference in GEM-Br reaction rates, result in significant differences in the springtime gross deposition of Hg simulated by GRAHM and

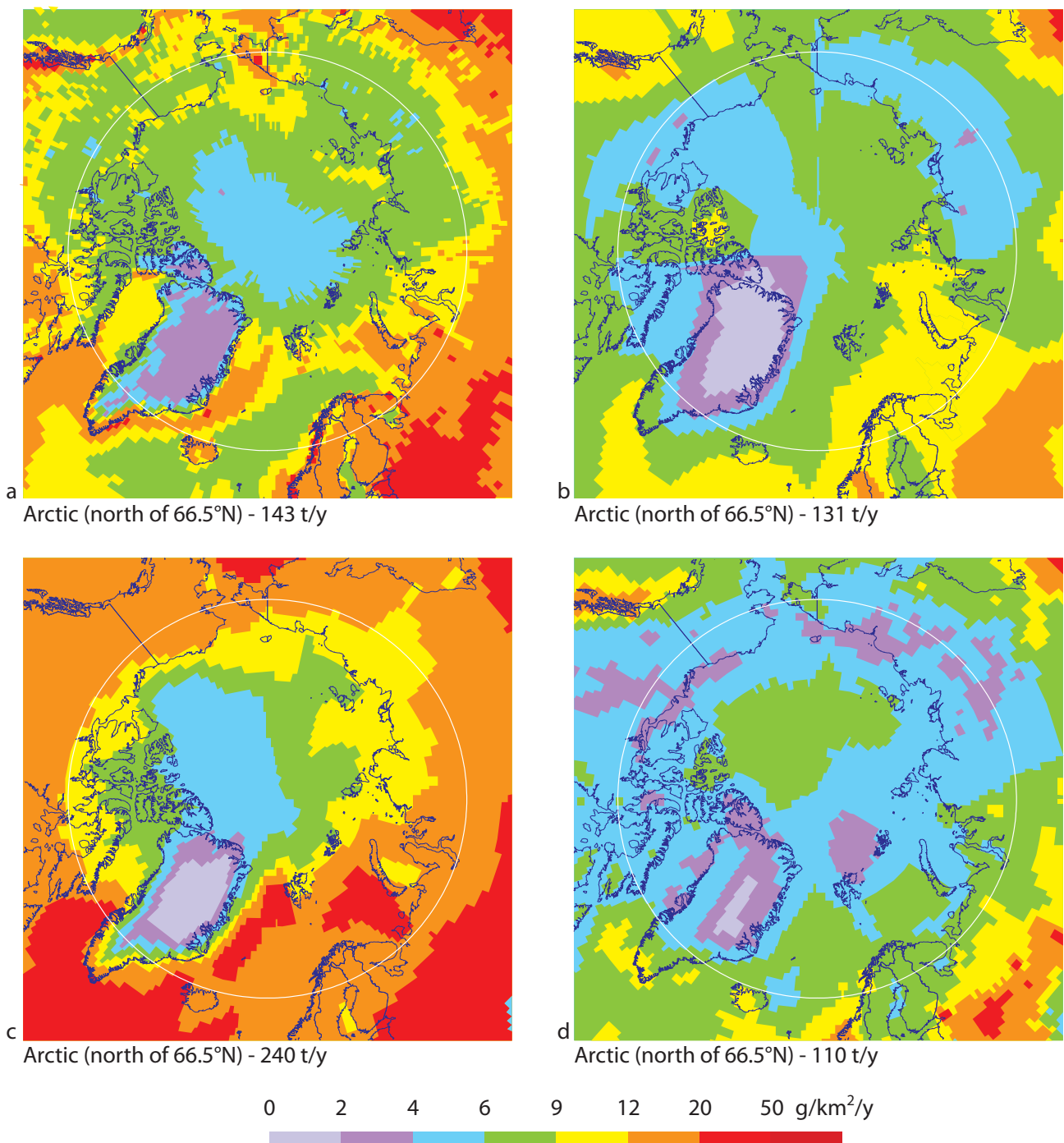


Figure 2.15. Spatial distribution of total mercury deposition to the Arctic simulated by (a) GRAHM (net), (b) GLEMOS (gross/net, see Table 2.6), (c) GEOS-Chem (gross), and (d) DEHM (gross/net, see Table 2.6) in 2005.

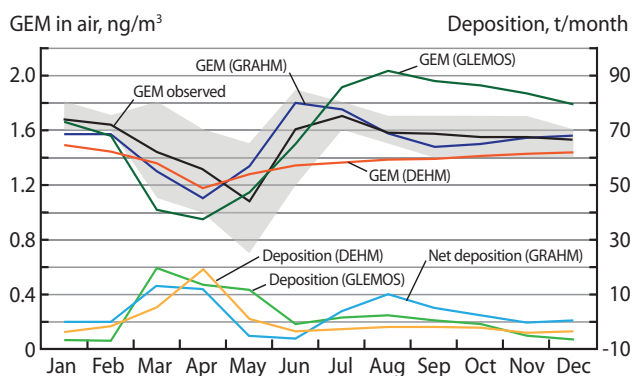


Figure 2.16. Monthly mean (north of 66.5° N) ambient concentrations of gaseous elemental mercury simulated by GRAHM, DEHM and GLEMOS and observed mean concentrations at six Arctic sites: Barrow, USA; Alert, Canada; Station Nord, Greenland; Ny-Ålesund, Norway; Andoya, Norway; Amderma, Russia (left scale). Total monthly deposition and net deposition simulated respectively by GRAHM, DEHM and GLEMOS (right scale). Negative deposition indicates higher re-emission than deposition.

GEOS-Chem. However, the deviations are less pronounced in net deposition estimates from these models.

Figure 2.16 shows average monthly means of GEM ambient concentrations and deposition fluxes from DEHM, GRAHM and GLEMOS within the Arctic Circle along with measured monthly mean GEM concentrations estimated from six measurements sites (Barrow, USA; Alert, Canada; Station Nord, Greenland; Ny-Ålesund, Norway; Andoya, Norway; Amderma, Russia). The error bars show the extreme values of monthly means at the six sites. It should be noted that all measurement sites are coastal, and different years are combined to arrive at the measured seasonal cycle (some sites did not report data for all months; Durnford et al., 2010). The yearly averaged GEM concentrations for GRAHM, GLEMOS, DEHM and observation are 1.47, 1.61, 1.37 and 1.52 ng/m<sup>3</sup>, respectively. The model-estimated mean GEM concentrations and the seasonal cycles in the Arctic are well represented by the observed GEM concentrations at the six Arctic measurement sites, which suggests that similar Hg processes are occurring throughout the Arctic region.

The yearly net deposition fluxes for the four models (GRAHM, GLEMOS, DEHM, GEOS-Chem) in the Arctic are, respectively, 143, 131, 110 and 80 t/y (Table 2.6). The models estimate mean GEM concentration in the Arctic within a factor of 1.2, however, the annual accumulation of Hg in snow estimated by the models varies by a factor of 1.8. One of the major constraints used in all the Hg models, is the observed surface GEM concentration. Therefore close inter-model agreement of GEM concentration is not surprising. The uncertainties in Hg emission fluxes and removal rate constants have led to the inclusion of different plausible representations of these processes in the models so that observed GEM air concentrations can be reproduced. However, the differences in removal rate constants and the underlying parameterizations result in a relatively larger spread in model estimates of net deposition fluxes.

A few instrument-based wet Hg flux datasets are available to help constrain the model deposition estimates. These are from sub-Arctic precipitation collection stations at Churchill, Manitoba, Fort Vermilion, Alberta (a northern boreal forest station; Sanei et al., 2010), and Kodiak, on the Pacific coast of Alaska (Mercury Deposition Network – MDN; [\[sws.uiuc.edu/mdn\]\(http://sws.uiuc.edu/mdn\)\). Gross wet deposition fluxes from these stations were compared to model estimates \(GEOS-Chem and GRAHM\) at these sites \(Sanei et al., 2010\). The modeled wet Hg fluxes for these three sites ranged from 2.1 to 4.1 µg/m<sup>2</sup>/y compared to measurements of 0.54 to 5.3 µg/m<sup>2</sup>/y. The model estimates were closest to observed fluxes at Kodiak \(GEOS-Chem -47% and GRAHM +23% compared to measurements\). The largest discrepancy between observations and model estimates was at Churchill, where intense and recurring AMDEs were found to occur with springtime snow Hg levels temporarily reaching over 100 ng/L \(Kirk et al. 2006\). Both the wet deposition measurements by Sanei et al. \(2010\), and the earlier atmospheric and snow monitoring of AMDEs by Kirk et al. \(2006\), were carried out at the Northern Studies Centre near the western Hudson Bay shoreline. Here, GEOS-Chem and GRAHM overestimated the measured fluxes by 4.0–7.6 times and 6.5 times, respectively, and no evidence of elevated Hg concentrations or fluxes in precipitation was detected during springtime. Lu et al. \(2001\) found that the eastern shore of Hudson Bay exhibited almost two times higher Hg concentrations in snow compared to sites on the western shore. Tarasick and Bottenheim \(2002\) examined the frequency of ODEs that are highly correlated to AMDEs during spring. The authors found that severe ODEs occurred frequently at Alert, Eureka and Resolute, however, at Churchill such events were found less frequently. Another possible explanation for the model/measurement differences is that the model estimates represent average fluxes within a grid cell defined by the resolution of each model. The spatial resolution of the two models may not have been high enough to adequately resolve the strong gradient in AMDE-related processes in this region. Kirk et al. \(2006\) measured high concentrations of Hg in snow during AMDEs and Sanei et al. \(2010\) measured low wet deposition fluxes at Churchill. However, the relative contribution of wet and dry deposition at Arctic sites including Churchill is essentially unknown. Uncertainties in partitioning of dry and wet deposition in the models could thus be another source of discrepancies between measured and modeled estimates of wet deposition at Churchill. Dry deposition flux measurements and more wet deposition measurements are required to evaluate the models and the impact of AMDEs in the Arctic. Sanei et al. \(2010\) also found that the models' wet deposition estimates were within 5% of measured fluxes at southern Alberta MDN stations where annual fluxes were up to 10 times higher than at the sub-Arctic sites. Similarly, Travníkov et al. \(2010\) compared wet deposition estimates from five global/hemispheric-scale models with measured fluxes at MDN sites across temperate North America. They reported that the model predictions were within a factor of 2 of observed fluxes at 57% to 91% of the MDN sites.](http://nadp.</a></p>
</div>
<div data-bbox=)

Analysis of the sources of atmospheric Hg deposited in the Arctic was performed by estimating the contribution from eight source regions (shown in Figure 2.17) covering most of the global anthropogenic emissions, using GRAHM, GEOS-Chem and GLEMOS. Total anthropogenic Hg emissions and percentages to the global anthropogenic emissions in these regions for 2005 (AMAP/UNEP, 2008) are indicated in Figure 2.17. GRAHM and GLEMOS also estimated separately the contributions from combined natural sources and re-emissions from these regions. GEOS-Chem estimated the deposition contribution from combined recent anthropogenic emissions

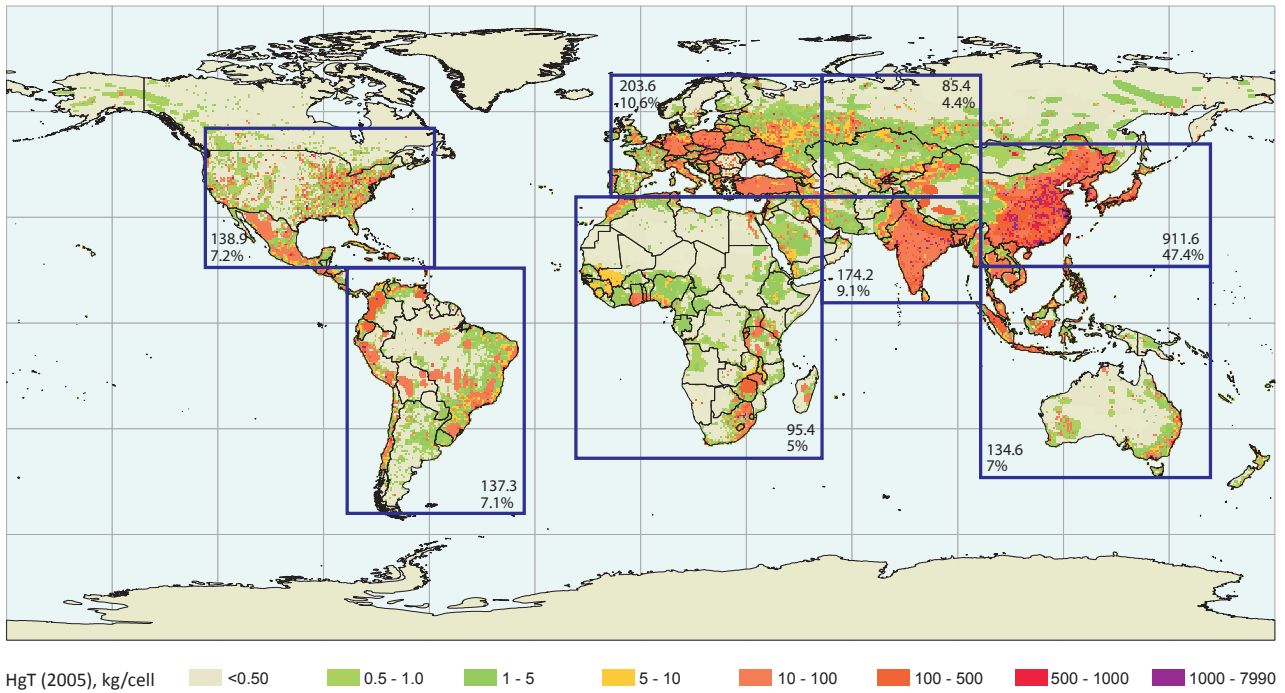


Figure 2.17. Location of source regions considered in the study, plus total anthropogenic emissions (t) and percentage global anthropogenic emissions of Hg in these regions for 2005.

and re-emissions from the eight source regions. All three models estimated the total contributions from global recent anthropogenic emissions (GEOS-Chem: anthropogenic and terrestrial re-emissions), oceanic emissions and terrestrial emissions (GRAHM and GLEMOS: natural and re-emissions; GEOS-Chem: natural emissions).

Figure 2.18 presents the model estimated contributions as well as total contributions from anthropogenic, terrestrial and oceanic emissions in 2005. The largest anthropogenic contribution is from East Asia followed by Europe, Central and South Asia, and North America. The most striking results of this analysis are that model estimates are close to each other with respect to the deposition contributions from recent anthropogenic emissions, and that the largest differences between model estimates of Arctic deposition are from the global natural sources and re-emissions. These results indicate that the largest differences in the model estimates of total deposition to the Arctic are due to the quantitative and spatial differences in natural emissions and re-emissions of Hg used by different models. The re-emissions estimates for Europe, North America and East Asia are significantly higher in GRAHM than in GLEMOS, which results in GRAHM estimating a larger overall contribution from these regions. GLEMOS and GEOS-Chem both included higher overall gas phase oxidation rates compared to GRAHM, which resulted in slightly shorter life times of Hg simulated by their models. On the contrary, a higher Br oxidation rate is used in GRAHM compared to GLEMOS and GEOS-Chem, leading to markedly higher gross deposition estimates by GRAHM which is mostly compensated by higher re-emission flux from the cryosphere. Natural and revolatilized emissions from land and ocean in GEOS-Chem are at least 50% higher (Table 2.6) than in GRAHM and GLEMOS, resulting in notably higher deposition contributions from these sources to the Arctic in GEOS-Chem. Overall, GRAHM estimates the highest contribution from natural sources and re-emissions

over land (anthropogenic: 29%; terrestrial: 41%; ocean: 30%), while GLEMOS estimates the highest contribution from ocean (anthropogenic: 31%; terrestrial: 33%; ocean: 36%). Since the GEOS-Chem anthropogenic estimate includes terrestrial re-emission, it is not possible to estimate the contribution from terrestrial and oceanic emissions separately for GEOS-Chem (anthropogenic and re-emission: 32%; terrestrial natural: 29%; ocean: 39%). Based on the source attribution results from the models, the deposition input of Hg to the Arctic is found to be most efficient for emissions from Russia and Europe, followed by North America, East Asia, South Asia, Australia, South America and Africa.

Figure 2.19 depicts model ensemble average spatial distribution of the deposition contribution from four major source regions: Europe, North America, East Asia, and South

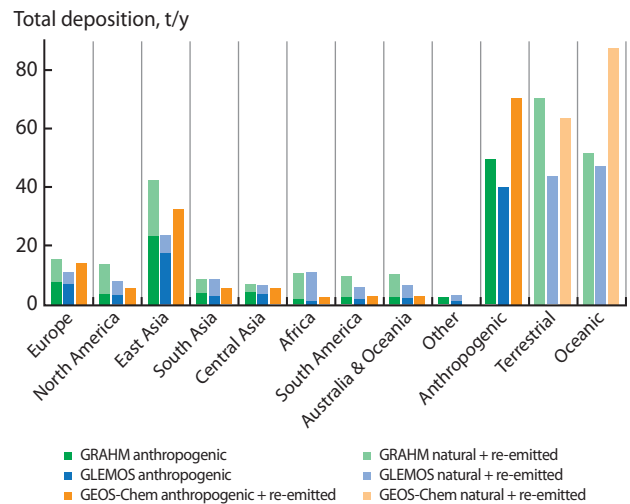


Figure 2.18. Contribution of the source regions to mercury deposition to the Arctic in 2005.

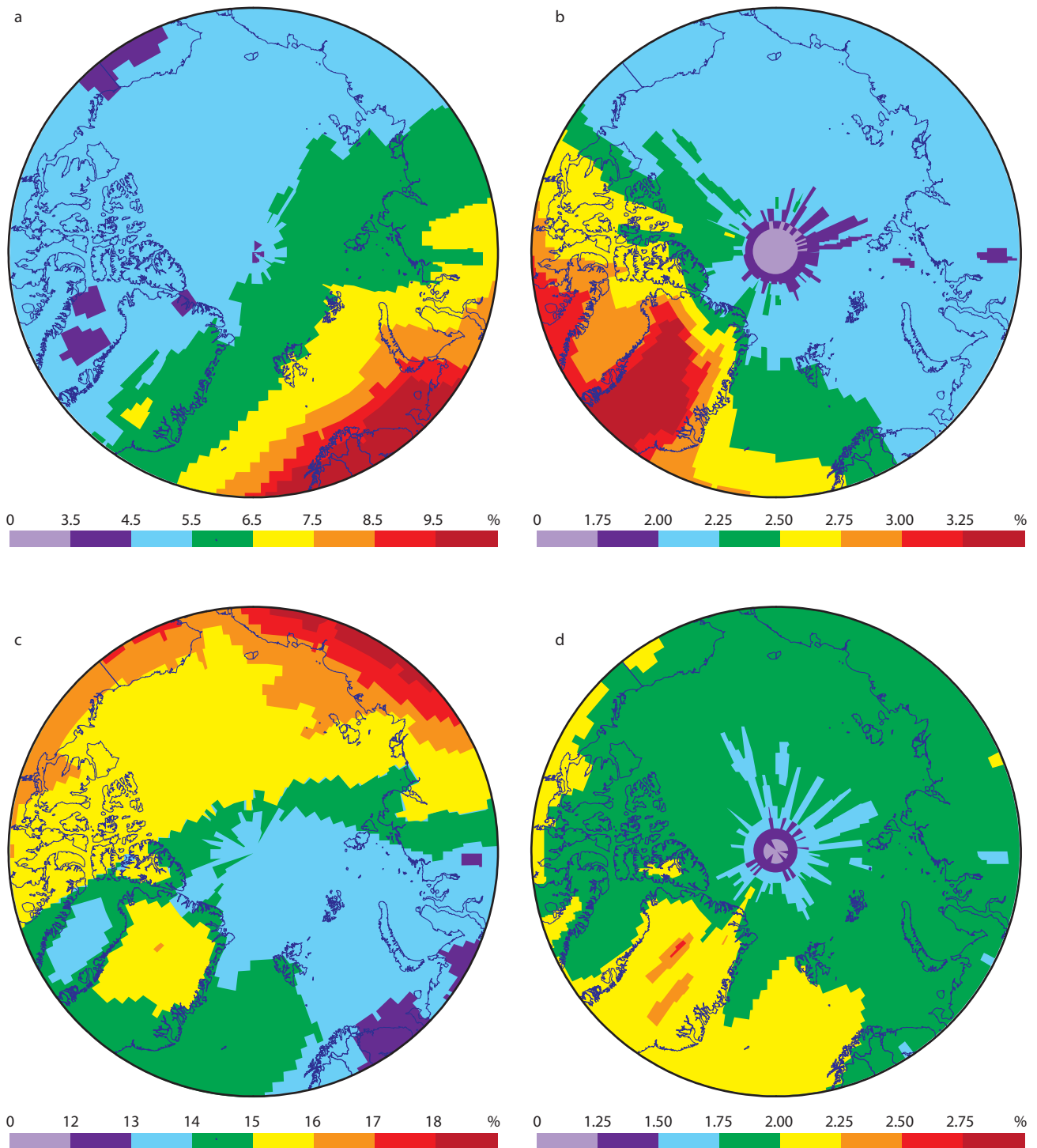
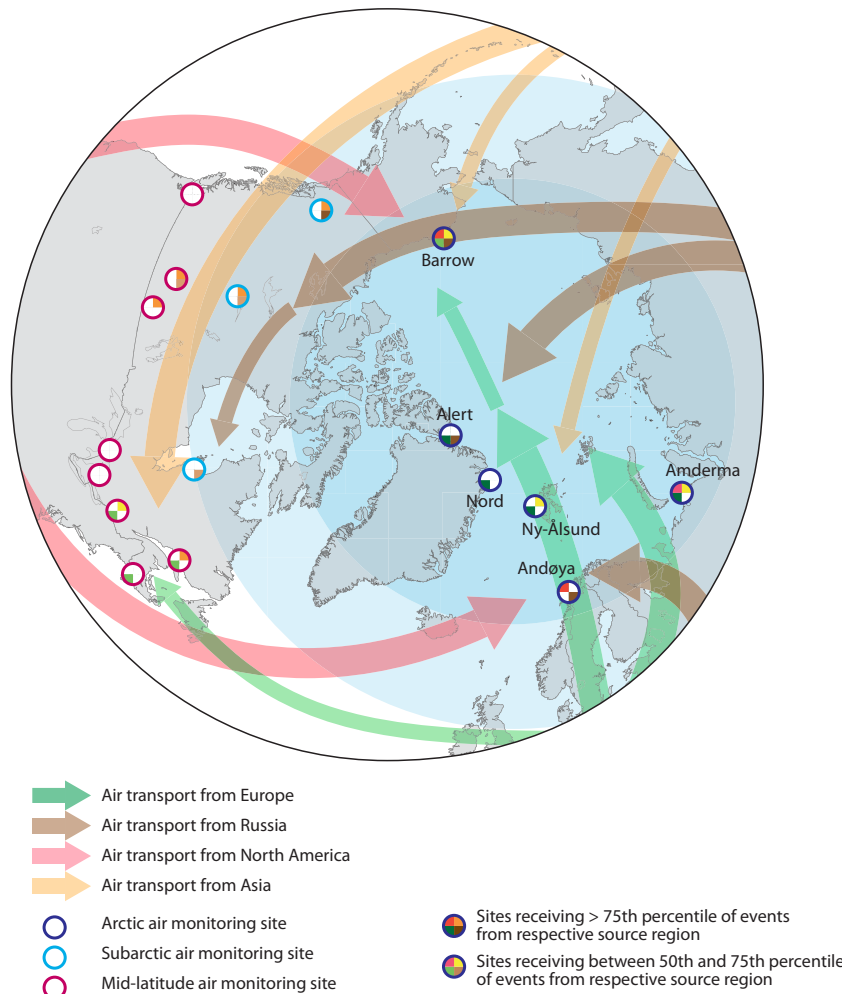


Figure 2.19. GLEMOS, GEOS-Chem and GRAHM model ensemble-mean spatial distribution of mercury deposition contribution to the Arctic from (a) Europe, (b) North America, (c) East Asia and (d) South Asia in 2005.

Asia. Since the lifetime of GEM in the atmosphere is between six and 24 months, the preferential long-range transport pathways from given source regions to the Arctic have a small impact on regional distribution of GEM transport and deposition to the Arctic. However as shown here, the North American and East Asian impact is somewhat higher in the western hemisphere, whereas the South Asian impact is slightly higher over Greenland and the adjacent ocean. European sources are closer to the Arctic therefore the regional variability of Hg contribution from this region is higher. These results suggest that relative changes in Hg emissions in these regions could

affect the atmospheric deposition differentially in the Arctic. For example, increasing emissions in East Asia could increase deposition in the Canadian Arctic offsetting the decrease coming from reductions in North American emissions. Alternatively, a decrease in European emissions could decrease the deposition in the European Arctic in spite of increasing emissions in East Asia. Relative changes in Hg levels in the Arctic as a result of recent changes in emissions are discussed in Section 2.6.1.3. The main Hg transport pathways in the Arctic, Sub-Arctic and mid-latitudes from the major emission regions were analyzed by Durnford et al. (2010) based on an analysis of

Figure 2.20. Dominant air transport pathways for mercury into the Arctic from major source regions, with an indication of the contribution from these source regions at specific monitoring locations. Source: after Durnford et al. (2010).



long-range transport events throughout the year, and on wind patterns that are shown in Figure 2.20. The figure identifies the transport pathways and the maximum, above the 75th percentile and between the 75th percentile and the median number of long-range transport events impacting on the Hg air measurement sites from Asia, North America, Russia and Europe. The study concluded that a higher percentage of long-range transport events are directed toward the Arctic from Europe and Russia compared to Asia and North America.

#### 2.6.1.2. Uncertainties associated with Arctic deposition estimated by atmospheric models

The two most fundamental parameters that determine the exchange of Hg between the Earth's surface and the atmosphere, in areas remote from sources, are the airborne emissions of GEM, and its overall oxidation rate. Currently, estimates of anthropogenic emissions are considered to be far more reliable (Section 2.2) than estimates of the natural and revolatilized emissions of GEM from terrestrial and ocean surfaces, which are presently highly uncertain (Section 2.3). The latter emissions are roughly half to two-thirds of total global GEM emissions and therefore represent a significant source of uncertainty in the models. Uncertainty in the speciation of Hg emission has a profound impact on the simulated Hg deposition since Hg(0) is subject to long-range transport, while RGM and particulate Hg (to a lesser extent) deposit rapidly near emission sources.

Another major limitation of the current atmospheric Hg models is uncertainty in the chemical speciation and kinetics of Hg species in air (Section 2.5). These are currently extrapolated from limited laboratory investigations. The uncertainties in the gaseous Hg chemistry are mainly associated with the reported kinetic constants, and the lack of deterministic product identification of Hg reaction. The existing Hg kinetic parameters for gas and aqueous phases, obtained from theoretical calculations and laboratory measurements, vary significantly, and the application of these data to the real atmosphere has been questioned (Calvert and Lindberg, 2005).

Given both that emissions and atmospheric oxidation rates of GEM have significant knowledge gaps, the models must rely upon observational data constraints to ascertain the appropriateness of parameterizations of Hg processes. However, GEM surface air measurements and wet deposition fluxes, mostly from mid-latitude North America and Europe, are almost the only reliable sources of observational data available to date. Measurements of oxidized Hg concentrations and dry deposition fluxes are severely limited and highly uncertain. In addition, present-day techniques cannot determine the speciation of oxidized Hg. The uncertainties, particularly in natural and re-emitted Hg fluxes (see Table 2.5), chemical mechanisms, reaction rates, speciation and GEM dry deposition could be considered in generally descending order in models. Other important sources of uncertainties are associated with the lack of knowledge of seasonal variation of anthropogenic

emissions, scavenging characteristics of Hg in liquid and solid condensate, precipitation rates and model resolution.

Large uncertainties both in Hg emissions and chemistry on the one hand and lack of adequate and reliable observations on the other, lead to a range of representations of non-anthropogenic Hg emissions, chemical mechanisms, Hg speciation and dry deposition in the models (Table 2.6). The four models applied to Arctic deposition and source attribution represent the full spectrum of parameters related to Hg processes. At the same time, all the models are constrained with common sets of Hg measurements. Therefore these models represent an ensemble that together provides a reasonable measure of the sensitivity of deposition estimates to various configurations and parameters of Hg processes available in the literature.

### 2.6.1.3. Impact of changing anthropogenic emissions from 1990-2005 on Arctic atmospheric mercury inputs

One of the measures of the impact of changes in Hg emissions worldwide is the temporal changes in atmospheric Hg levels in the Arctic. Long-term monitoring records for GEM concentrations at several Arctic sites have been analyzed in Section 2.5.2. However, it is challenging to relate the observed trends to the heterogeneous variations in anthropogenic Hg emissions on the globe. At the same time as anthropogenic emissions have changed, the observed changes in Arctic Hg may be also impacted by variations in weather patterns and in natural and re-emitted emissions, atmospheric chemical composition, land-use and climate. Modeling the impact of these factors independently and in combination on global Hg transport can illuminate the relationship of these changes to the measured trend in Hg levels in the Arctic.

Modeling studies have been conducted using global Hg inventories for 1990, 1995, 2000 and 2005 that were previously developed by AMAP. Recently, AMAP re-analyzed the 1990 to 2005 global anthropogenic emission inventories and developed more comparable historical inventories that are better suited for modeling the impact of changing Hg emissions in the Arctic over recent decades. The re-analyzed inventories use a common methodology and a more consistent information base for estimating certain emissions. Details are discussed in

Section 2.2.2. Briefly, emissions in Europe and North America declined most rapidly from 1990 to 2000 and declined only slowly from 2000 to 2005 (see Figure 2.8). The emissions from other continents, most notably Asia, steadily increased from 1990 to 2005. Overall, global anthropogenic Hg emissions declined from 1990 to 1995 by 7.8% and increased between 1995 and 2000, and 2000 and 2005, by 0.3% and 5.6%, respectively.

As part of the current Assessment the GLEMOS, DEHM and GRAHM models were applied to assess the impact of changing anthropogenic emissions since 1990 on Hg concentrations in and deposition from the Arctic atmosphere. All three models used the four new emission inventories (1990 to 2005) while keeping the meteorology and all other variables identical in the model runs. Table 2.7 and Figure 2.21 illustrate the average simulated changes in Hg surface air concentrations and net deposition fluxes in the Arctic from 1990 to 2005.

The model results showed a decline in average surface air concentrations of GEM in the Arctic between 1990 and 1995 that was roughly half of the decline in anthropogenic emissions over this period, because over half of the total global GEM emissions are from natural and re-emission sources. Although anthropogenic emissions increased between 1995 and 2000, the simulated GEM concentrations and deposition in the Arctic and sub-Arctic continued to decline until 2000, mainly due to the larger impact of reductions in European and North American emissions. Durnford et al. (2010) found that the relative efficiency of Hg transport to the Arctic from Europe was higher than from Asia. For a similar reason, GEM concentrations and deposition in the Arctic increased more slowly from 2000 to 2005 than the increase in global emissions because of the off-setting effect of decreasing European and North American emissions. The model simulations also pointed to regional differences within the Arctic in response to changes in emissions from global industrial sources. The smallest reductions were predicted to occur in the North American Arctic, because of the impact of increasing emissions from Asia on this region that offset the emission reductions in North America. Further modeling studies are needed to investigate the potential impact of coincidental changes in meteorological, environmental and climatic variables (listed earlier) on the temporal trends of Hg in the Arctic atmosphere.

Table 2.7. Annual mercury deposition from 1990 to 2005 and percentage change relative to preceding year (1995 vs 1990, 2000 vs 1995, 2005 vs 2000) for various Arctic and Sub-Arctic regions.

Mercury emission and deposition	1990		1995		2000		2005	
	t/y		t/y	%	t/y	%	t/y	%
Global anthropogenic mercury emissions	1967.27		1813.88	-7.8	1818.57	0.3	1920.57	5.6
<b>Arctic 66.5° N – 90° N</b>	<b>133.12</b>		<b>122.79</b>	<b>-7.8</b>	<b>117.39</b>	<b>-4.4</b>	<b>119.34</b>	<b>1.7</b>
European Arctic 10° W – 60° E	37.04		33.33	-10.0	31.36	-5.9	31.71	1.1
Asian Arctic 60° E – 170° W	49.41		44.82	-9.3	42.53	-5.1	43.46	2.2
North American Arctic 170° W – 10° W	45.95		43.87	-4.5	42.76	-2.5	43.44	1.6
<b>Sub-Arctic 60° N – 66.5° N</b>	<b>134.32</b>		<b>114.86</b>	<b>-14.5</b>	<b>105.40</b>	<b>-8.2</b>	<b>106.94</b>	<b>1.5</b>
West European sub-Arctic 10° W – 20° E	16.03		13.57	-15.4	12.34	-9.1	12.12	-1.7
East European sub-Arctic 20° E – 60° E	30.08		22.95	-23.7	19.19	-16.4	19.49	1.6
West Asian sub-Arctic 60° E – 100° E	19.57		16.16	-17.4	14.31	-11.4	14.73	3.0
East Asian sub-Arctic 100° E – 170° W	25.87		21.21	-18.0	19.45	-8.3	20.04	3.1
West North American sub-Arctic 170° W – 100° W	17.51		16.95	-3.2	16.62	-1.9	16.83	1.2
East North American sub-Arctic 100° W – 10° W	25.54		24.14	-5.5	23.50	-2.6	23.78	1.2

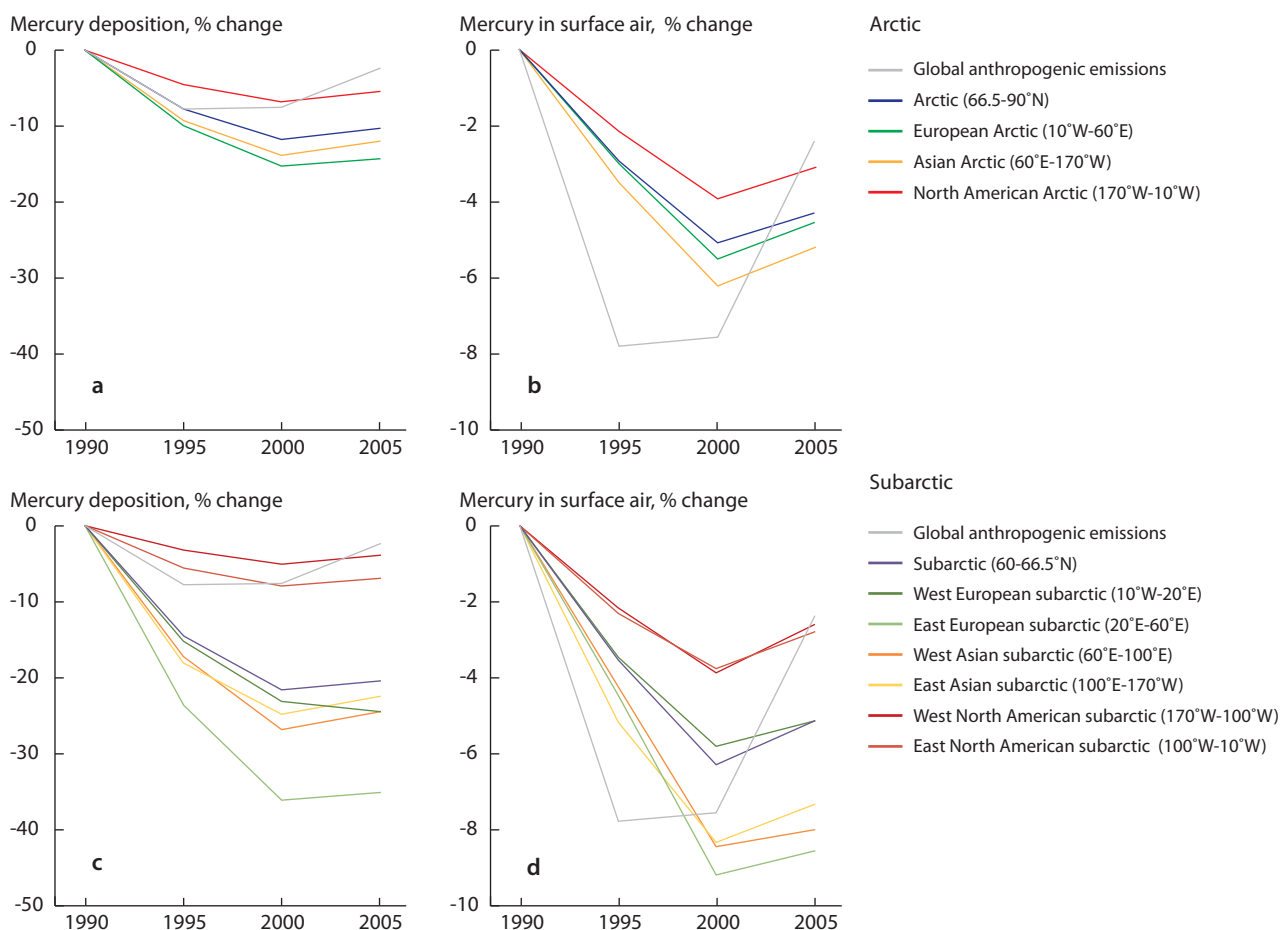


Figure 2.21. Relative change in annual mercury deposition between 1990 and 2005 in (a) Arctic and (c) sub-Arctic regions, and relative changes in surface air mercury concentrations in (b) Arctic and (d) sub-Arctic regions.

### 2.6.2. Field observations of re-emission of deposited mercury from snow surfaces

Mercury transformations at the interface between air and snow are a key component of the Arctic Hg cycle because atmospheric deposition is a major source of Hg (Skov et al., 2004; Ariya et al., 2004) and much of the Arctic surface is covered by snow for most of the year. The fate of Hg in snow is of fundamental importance because of its potential to enter aquatic ecosystems during spring melt and stimulate methylmercury production, followed by its bioaccumulation in food webs (Lindberg et al., 2002; Ebinghaus, 2008). Snow surfaces and ice crystals can become concentrated with Hg following the rapid oxidation of GEM during springtime AMDEs, reaching THg levels as much as 100 to 1000 ng/L (Lu et al., 2001; Kirk et al., 2006; Douglas et al., 2008; Johnson et al., 2008; Dommergue et al., 2010).

Freshly deposited Hg on snow is highly reactive (Lalonde et al., 2002), and a large portion of the Hg deposited during AMDEs is quickly revolatilized (re-emitted) to the atmosphere because of photo-reduction of Hg(II) to GEM within the surface snowpack (Lalonde et al., 2002; Poulain et al., 2004). A review of studies on snow Hg concentrations suggests that this rapid loss in surface snow is a common feature across the circumpolar Arctic (Table 2.8 and Figure 2.22). Approximately 80% of newly deposited mercury from AMDEs is typically lost from the snow surface after two days or longer. GEM flux

measurements at the snow-air interface support the hypothesis that Hg loss is primarily due to re-emission to the atmosphere (Lahoutifard et al., 2005; Ferrari et al., 2005; Brooks et al., 2006; Johnson et al., 2008; Dommergue et al., 2010), although some loss may also result from movement into deeper layers of the snowpack or horizontal transfer from blowing snow.

Certain environmental conditions can promote retention of Hg within the snowpack. Low light energy, particularly in layers deeper than 10 cm, may prevent photo-reduction (King and Simpson, 2001). Moreover, changes in the incoming light energy regime can result in re-oxidation of the newly produced Hg(0) (Poulain et al., 2004). The presence of halogens in snow can help retain Hg by favoring a photo-oxidation reaction (Amyot et al., 2003), and indeed, elevated snow Hg concentrations are more often found in Arctic ocean or coastal environments where a deposition of sea-salt may be expected (Douglas and Sturm, 2004; Poulain et al., 2007a; St. Louis et al., 2007). Conversely, these higher concentrations may occur primarily because AMDEs are a result of photochemical reactions involving marine halogens and ozone (Lindberg et al., 2002; Simpson et al., 2007a). Burial through snow accumulation, sublimation, condensation and ice layer formation are other processes that promote retention of Hg in the snowpack (Douglas et al., 2008).

While deposition occurs at the snow surface, Hg can also be redistributed within the snow accumulation. Migration of GEM within the snowpack and subsequent oxidation could result in accumulation of Hg within deeper layers (Dommergue et al.,

Table 2.8. Percentage loss of total mercury (THg) concentrations in surface snow shortly following atmospheric mercury depletion events (AMDEs) at various Arctic locations. Concentrations are mean  $\pm$  1 SD, maximum (during AMDE only), range or single observation depending on the study (n in parentheses). Percentage loss of snow THg determined by measurements of gaseous elemental mercury (GEM) fluxes is also provided as a comparison.

Location	Date of AMDE	Sampling site	THg in snow during and after AMDE, ng/L		Number of days after AMDE	Percentage loss in snow	Depth sampled in snowpack, cm	Source
			During	After				
Alert, Canada	11-14 April 2002	Over sea ice	5.7 (1)	~1 (1)	1	~82	surface	St. Louis et al., 2005
	23-25 April 2002	Over land	7.3 (1)	<2 (1)	5	>73	surface	St. Louis et al., 2005
Barrow, Alaska	May 2000	Over land	>90 (1)	<20 (1)	6 or more	<b>92</b> <sup>a</sup>	0-10	Lindberg et al., 2002
	22-31 March 2006	Site 1, over land	194 $\pm$ 22 (14)	53 (1)	2	73	0-1	Johnson et al., 2008
		Site 2, over land	147 (17)	41 (1)	2	72	0-1	Johnson et al., 2008
Churchill, Canada	19 March to 3 June 2004 <sup>b</sup>	Over sea ice	67.7 $\pm$ 97.7	36.5 $\pm$ 16.3	1	46	surface	Kirk et al., 2006
		Over sea ice	67.7 $\pm$ 97.7	15.8 $\pm$ 8.1	2	77	surface	Kirk et al., 2006
		Over sea ice	67.7 $\pm$ 97.7	22.3 $\pm$ 12.3	3	67	surface	Kirk et al., 2006
		Over sea ice	67.7 $\pm$ 97.7	4.3 $\pm$ 1.9	4 or more	94	surface	Kirk et al., 2006
Kuujuarapik, Canada	10-11 April 2002	Over land	~20-24 (4)	17.2 (2)	1	~14-28	surface	Dommergue et al., 2003b
		Over land	~20-24 (4)	2.3 (2)	1.5	~89-90 <sup>a</sup>	surface	Dommergue et al., 2003b
	13 March 2004	Over land	12-16 (6)	10-16 (6)	2	~0 <sup>c</sup>	0-10	Constant et al., 2007
	16 March 2004	Over land	~12 (2)	~3 (2)	0.5	<b>78</b>	0-10	Constant et al., 2007
Ny-Ålesund, Norway	21-23 April 2002	Over land	~40 (1) <sup>d</sup>	<10 (1)	6	>75	surface	Sommar et al., 2007
	24-27 April 2005	Over land	44.1 $\pm$ 19.0 (6)	28.4 $\pm$ 18.5 (15)	7 or more	36 <sup>e</sup>	surface	Ferrari et al., 2008
Resolute, Canada	7-14 May 2003	Over land	29.2 $\pm$ 1.5	<15	3	>49	0-10	Lahoutifard et al., 2005
	7 June 2003	Over land	17.7 $\pm$ 7.8 (3)	1.5 (3)	2	<b>92</b>	0-1	Poulain et al., 2004
			GEM fluxes between air and snow ( $\mu\text{g Hg}/\text{m}^2$ )					
			Deposition	Re-emission				
Barrow, Alaska	25 March to 7 April 2003 <sup>b</sup>	Over land	1.7	1.0		59	n.a.	Brooks et al., 2006

Percentage loss values in bold were calculated by the authors of the respective study. na; not applicable. <sup>a</sup> Losses during snowmelt; <sup>b</sup> multiple AMDEs occurred between those dates; <sup>c</sup> essentially no loss in snow THg concentration was observed; <sup>d</sup> maximum snow THg concentration measured during GEM recovery phase (24 April 2004); <sup>e</sup> Ferrari et al. (2008) reported an 80% loss relative to pre-AMDE THg concentrations in snow (instead of relative to mean THg concentration during the AMDE as calculated here).

2003a; Faïn et al., 2006a,b). Melt events may redistribute Hg toward deeper layers away from the high energy surface of the snowpack. A review of Arctic studies on the depth distribution of THg within the snowpack suggests that the highest THg concentrations are most commonly found in the surface layer (Table 2.9). However, the middle stratum and depth hoar can also be dominant reservoirs of Hg in some settings, emphasizing the fact that post-depositional processes over the entire depth of the snowpack may influence Hg accumulation.

The onset of spring melt results in a rapid flushing of THg from the snowpack; Hg(II) is transported by melt waters and photo-reduction also returns some of the Hg to the atmosphere (Lindberg et al., 2002; Dommergue et al., 2003b; Aspino et al., 2006). Studies of THg concentrations in snowmelt water in the Canadian and Greenland Arctic generally display a range from 0.3 to 10 ng/L, with an average of about 3 ng/L (Outridge et al.,

2008), although high Hg concentrations may occur briefly in the surface meltwater from a snowpack during the earliest melt period (e.g., up to 24 ng/L for 1 day; Dommergue et al., 2010).

A few studies have estimated the net impact of snowmelt Hg loadings from springtime AMDEs on receiving waterbodies. At Ny-Ålesund (Svalbard, Norway), Dommergue et al. (2010) found that because most Hg deposited on snow was photo-reduced and re-emitted back to the atmosphere, snowmelt contributed 8-21% of the annual THg loading to a fjord. Similarly, Kirk et al. (2006) estimated that AMDEs resulted in only a small net loading of Hg to Hudson Bay, Canada (equivalent to  $2.1 \pm 1.7$  mg/ha;  $0.21 \pm 0.07$   $\mu\text{g}/\text{m}^2$ ) because of high re-emission rates. St. Louis et al. (2007) estimated snowpack contributions of 5.2 mg/ha for the Canadian High Arctic and concluded that Arctic snow contributes relatively little to marine pools of Hg. These observations suggest that, for at least most marine waters, the

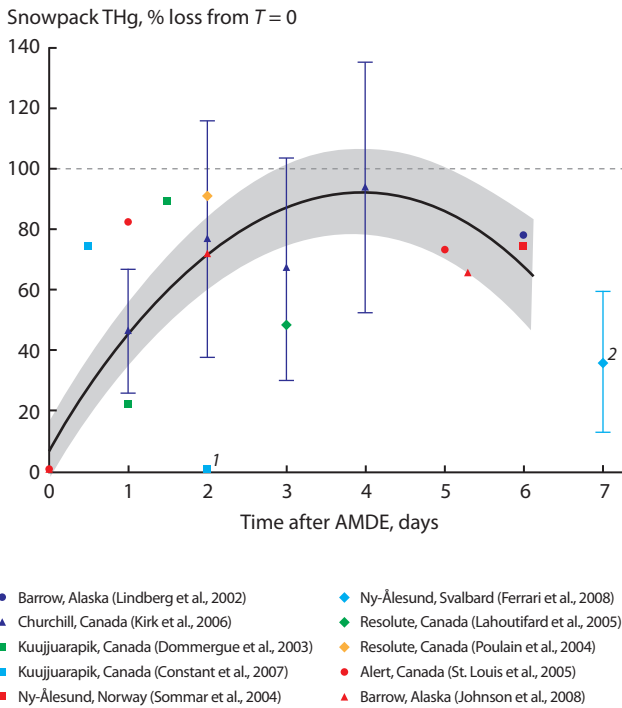


Figure 2.22. Rate of total mercury loss from Arctic surface snow (0 to 10 cm depth) after atmospheric mercury depletion events (AMDEs). (Data from Kirk et al. (2006) represent mean  $\pm$  1 SD, for other studies, the median values are used. Polynomial quadratic regression:  $\text{THg (ng/L)} = 5.77 + 44.7x - 5.75x^2$  ( $r^2 = 0.78$ ,  $p < 0.0001$ , total  $df = 26$ ); shaded area indicates 95% confidence intervals around regression. Data points 1 and 2 were excluded; 1: see note 'c' in Table 2.8., 2: see note 'e' in Table 2.8.).

overall contributions of Hg following springtime AMDEs are less significant than previously thought (e.g., Lu et al., 2001; Lindberg et al., 2002), probably because of the dominant effect of photo-reduction. However, there may be differences between different kinds of environments in the net snowmelt contribution. Poulain et al. (2007a) reported that surface seawater sampled from a sea-ice lead during the time of ice melt temporarily exhibited THg concentrations that were 5 to 10 times greater than those at depth. Photo-reduction is hampered in seawater due to its high halogen content and consequently once Hg(II) enters marine ecosystems it may have a longer residence time than in freshwater (Poulain et al., 2007b). It is also possible that Hg contained in marine snow and ice may be more directly available to ice algae communities that represent a key part of the Arctic marine food web.

## 2.7. Can atmospheric fate models reproduce historical mercury deposition rates recorded in sediments, peat or by instruments?

To understand future effects, it is necessary to understand past processes. Environmental archives provide a means of doing so, because they are widely believed to accurately preserve the deposition history of Hg through time, either as a direct record or modulated by some type of focusing. All environmental archives by their nature involve an annual or seasonal accumulation process, which allows a chronology to be

established. Studies on Hg deposition in environmental archives in the Arctic and sub-Arctic include records preserved in glacial ice and firn (perennial snowpack) (e.g., Faïn et al., 2006a,b, 2007, 2008, 2009b), lake sediments (Landers et al., 1995, 1998, 2008; Hermanson 1998; Bindler et al., 2001a,b; Lindeberg et al., 2006, 2007; Outridge et al., 2007; Muir et al., 2009), marine sediments (Siegel et al., 2001), and peat (Shotyk et al., 2003, 2005b; Givélet et al., 2004b; Bindler et al., 2005). Aside from lake sediments, there is limited spatial coverage across the Arctic of environmental archives, and the geographical representativeness of the other records is still under debate. Chronological resolution of the investigated archives was sometimes limited given the uncertainty associated with sampling and dating techniques.

Human activities have perturbed the natural biogeochemical cycling of Hg as well as other elements emitted through anthropogenic processes. It is essential that this perturbation is understood, so that future deposition and subsequent impacts given a warming climate and changing global atmospheric Hg concentrations may be reasonably predicted by atmospheric deposition models. This type of historical information is also required for effective environmental management (Hylander and Goodsite, 2006; Renberg et al., 2009), which requires a good knowledge of past accumulation rates as a basis for comparison with current accumulation rates and possibly future predictions given climate and global emission trends.

Owing to the paucity of real-time, instrumental atmospheric flux data for the Arctic, environmental archives of Hg deposition are particularly important sources of data for checking against atmospheric model outputs. There are advantages and limitations to any archive, and each type of archive should be seen as providing biogeochemical information that is supplementary and complementary to each other. This section attempts to address whether one, all, or any of the non-biological archives can accurately reproduce historical trends in Hg deposition in the Arctic, and if so, can atmospheric fate and transport models then reproduce these trends.

The trends in Arctic atmospheric Hg concentrations and deposition over recent decades represent the empirical basis for answering these questions. Recent work on GEM trapped in snow and firn layers at Greenland Summit (Faïn et al., 2009b) and a series of airborne particulate Hg samples collected at Resolute, Nunavut (Li et al., 2009) has now provided a database extending back several decades, while GEM monitoring at Alert, Nunavut, since 1995 (Temme et al., 2007) provides the longest, real-time instrumental dataset of GEM trends in the Arctic. Collectively, this body of work reveals that there was an approximate two-fold rise in atmospheric GEM concentrations before the 1970s, largely due to increased anthropogenic Hg emissions during the 20th century (Faïn et al., 2009b). Subsequently, a large-scale decline in atmospheric gaseous and particulate Hg levels occurred during the 1970s to 1990s in northern Canada and Greenland, probably due to implementation of air pollution regulations, especially on coal-fired power plants (Faïn et al., 2009b; Li et al., 2009). This decline is consistent with global emission inventories (Faïn et al., 2009b; see also Section 2.2.2). GEM concentrations in Greenland Summit snow, and in air at Resolute, have been largely stable or possibly slowly declining since the 1990s (Temme et al., 2007; Faïn et al., 2009b; see also Section 2.6.1).

Table 2.9. Comparison of total mercury (THg) concentrations in different layers of the snowpack (surface, middle stratum, depth hoar) at various Arctic locations. Observations are presented in order of increasing concentration (mean  $\pm$  1 SD, n in parentheses) in the surface layer.

Location	Date	Sampling site	THg in snow, ng/L			Rank of THg concentration in snow strata	Source
			Surface	Middle stratum	Depth hoar		
Resolute, Canada	14 June 2003	Over land	<1 (3)	<1 (6)	<1 (3)	---	Poulain et al., 2004
Resolute, Canada	9 June 2004	Over lake ice	0.9 $\pm$ 0.02 (3)	0.4-2.7 (6)	0.6 $\pm$ 0.4 (3)	M > S > D	Poulain et al., 2007a
Colville, Alaska	March/April 2002	Over land	1.1 $\pm$ 0.7 (3)	0.5 $\pm$ 0.2 (3)	0.8 $\pm$ 0.5 (3)	S > D > M	Douglas and Sturm, 2004
Council, Alaska	March/April 2002	Over land	1.4 $\pm$ 0.2 (3)	1.2 $\pm$ 0.2 (3)	1.0 $\pm$ 0.1 (3)	S > M > D	Douglas and Sturm, 2004
Selawik, Alaska	March/April 2002	Over land	1.4 $\pm$ 0.5 (3)	1.3 $\pm$ 0.0 (3)	1.7 $\pm$ 0.5 (3)	D > S > M	Douglas and Sturm, 2004
Brooks Range, Alaska	March/April 2002	Over land	1.7 $\pm$ 0.1 (3)	1.1 $\pm$ 0.2 (3)	1.0 $\pm$ 0.5 (3)	S > M > D	Douglas and Sturm, 2004
Resolute, Canada	9 June 2004	Over sea ice	1.8 $\pm$ 0.6 (3)	4.9 $\pm$ 0.5 (3)	45.2 $\pm$ 13.1 (3)	D > M > S	Poulain et al., 2007a
Axel Heiberg Island, Canada	16 May 2004	Over land	2.5 (1)	0.3 (1)	0.1 (1)	S > M > D	St. Louis et al., 2007
John Evans Glacier, Canada	10 May 2004	Over land	2.6 (1)	0.4 (1)	0.2 (1)	S > M > D	St. Louis et al., 2007
Allman Bay, Canada	10 May 2004	Over sea ice	3.6 (1)	0.3 (1)	0.6 (1)	S > D > M	St. Louis et al., 2007
Talbot Inlet, Canada	10 May 2004	Over sea ice	4.5 (1)	0.4 (1)	7.9 (1)	D > S > M	St. Louis et al., 2007
Alert, Canada	12 April 2002	Over sea ice	5.7 (1)	0.4 (1)	2.5 (1)	S > D > M	St. Louis et al., 2005
Kuujuarapik, Canada	14 April 2002	Over land	~6 (2)	2.6 (4)	~4 (2)	S > D > M	Dommergue et al., 2003b
Buchanan Bay, Canada	10 May 2004	Over sea ice	6.1 (1)	1.3 (1)	5.4 (1)	S > D > M	St. Louis et al., 2007
Alert, Canada	31 May 2004	Over land	6.2 (1)	1.2 (1)	1.4 (1)	S > D > M	St. Louis et al., 2007
Atkasuk, Alaska	March/April 2002	Over land	6.6 $\pm$ 0.2 (3)	3.3 $\pm$ 1.5 (3)	~1 (3)	S > M > D	Douglas and Sturm, 2004
Alert, Canada	25 April 2002	Over land	7.3 (1)	19.2 (1)	<2 (1)	M > S > D	St. Louis et al., 2005
Norwegian Bay, Canada	16 May 2004	Over sea ice	8.0 (1)	8.1 (1)	1.2 (1)	M > S > D	St. Louis et al., 2007
Kuujuarapik, Canada	6 April 2002	Over land	~10 (2)	14.3 (4)	~4 (2)	M > S > D	Dommergue et al., 2003b
Alert, Canada	22 April 2002	Over sea ice	11.1 (1)	21.1 (1)	1.3 (1)	M > S > D	St. Louis et al., 2005
Eureka Sound, Canada	16 May 2004	Over sea ice	15.9 (1)	1.4 (1)	9.8 (1)	S > D > M	St. Louis et al., 2007
Resolute, Canada	7 June 2003	Over land	17.7 $\pm$ 7.8 (3)	~2 (6)	<1 (3)	S > M > D	Poulain et al., 2004
Bay Fiord, Canada	16 May 2004	Over sea ice	19.8 (1)	18.1 (1)	48.6 (1)	D > S > M	St. Louis et al., 2007
Churchill, Canada	31 March, 16 April, 22-23 May 2004	3 sites over sea ice	21.4 $\pm$ 27.2 (9)	15.2 $\pm$ 13.8 (9)	10.6 $\pm$ 9.6 (9)	S > M > D	Kirk et al., 2006
Wellington Channel, Canada	16 May 2004	Over sea ice	66.4 (1)	3.3 (1)	2.3 (1)	S > M > D	St. Louis et al., 2007
Jones Sound, Canada	11 May 2004	Over sea ice	78.2 (1)	8.0 (1)	17.1 (1)	S > D > M	St. Louis et al., 2007
Makinson Inlet, Canada	10 May 2004	Over sea ice	150 (1)	253 (1)	281 (1)	D > M > S	St. Louis et al., 2007
Barrow, Alaska	June 2000	Over land	---	21 $\pm$ 10	50-90	D > M	Lindberg et al., 2002
No. observations with highest [THg] at:						surface	16
						middle stratum	5
						depth hoar	6

Concentrations in each layer were measured in the same snowpack on a single sampling date except observations at Churchill and Barrow which are means of multiple sampling dates and/or snowpacks.

With respect to Hg deposition data, at northern European stations a comparison of deposition fluxes for the period 1995-1998 with those for 1999-2002 showed a decrease of 10-30%, which was attributed to reduced emissions in industrial areas of Europe (Wängberg et al., 2007). In a more recent comparison between three time periods (1995-1998, 1999-2002, 2003-2006), which also included the Pallas station (northern Finland), no significant trends in TGM or bulk deposition of Hg were found at Pallas, consistent with the previously-discussed studies on GEM trends at Alert and Greenland Summit. A continued decrease in Hg in bulk deposition was however

found at most northern European stations, while trends in TGM were variable or insignificant (Wängberg et al., 2010). In North America, no deposition monitoring stations have been active in Arctic regions long enough to establish a time trend.

Major comparative studies have been conducted between instrument-based measurement of Hg deposition and atmospheric modeling results covering areas outside the Arctic (e.g., Bullock et al., 2008, 2009), discussion of which is beyond the scope of this report. To date, however, there has only been one such study relevant to the Arctic (Sanei et al., 2010). Sanei et al. (2010) reported wet deposition Hg fluxes

measured over two years using precipitation collectors operated at Churchill on Hudson Bay, and at a second site in the western Canadian boreal forest. Because of typically low precipitation rates, measured Hg fluxes (0.5 to 1.3  $\mu\text{g}/\text{m}^2/\text{y}$ ) at these sub-Arctic sites were lower than those reported for temperate North American stations and for a station at Kodiak, Alaska, recently established by the Mercury Deposition Network ([nadp.sws.uiuc.edu/mdn](http://nadp.sws.uiuc.edu/mdn)). GRAHM and GEOS-Chem model estimates for these locations were supplied by A. Dastoor (Environment Canada) and C. Holmes (Harvard University), respectively. For the Canadian sub-Arctic stations, both models consistently over-estimated wet Hg fluxes relative to field measurements. The largest discrepancy with both models was for Churchill, where AMDEs occur during spring (March to May; Kirk et al., 2006). Here, the model annual flux values were up to 7.6 times higher than measurements for GEOS-Chem, and 6.5 times higher for GRAHM. However, much better agreement was obtained for Kodiak, which experiences 4-fold higher annual precipitation rates (and an almost 10-fold higher annual Hg flux) than the Canadian sub-Arctic sites. GRAHM model wet flux estimates at Kodiak were only 23% higher than measured (based on 2007 modeled vs 2008 MDN measured data). GEOS-Chem gave an estimate 47% lower than measured at Kodiak.

GEOS-Chem is designed to resolve fluxes on relatively coarse, global scales, and is particularly not intended to provide accurate predictions for coastal sites such as Churchill (C. Holmes, Harvard University, pers. comm., Nov 11, 2009). Sanei et al. (2010) suggested that the closer agreement for the Kodiak and other MDN stations could be interpreted to mean that larger wet Hg fluxes, due either to elevated Hg concentrations or precipitation rates, may be modeled more accurately than are the fluxes in low precipitation, low Hg concentration settings such as the Canadian sub-Arctic. It is possible that precipitation type as well as amount may be an issue in relation to the model calculations. The relative scavenging effect of snow vs rain on the flux of atmospheric Hg is a research area needing attention.

In general, the snow and ice records have demonstrated the most consistent representations of historical Hg accumulation. However they are in air masses that are away from the coastlines and thus potentially not affected by AMDEs. They are also difficult to sample and analyze owing to their typically very low Hg concentrations. Sediments, whether lacustrine or marine, are the archives with the greatest spatial resolution so far in the Arctic, but physical, chemical and biological sources of perturbation to the signal that they present are a source of great discussion in the scientific community. Efforts are being made to better address issues such as focusing of Hg (Van Metre et al., 2009), as the lake dataset may provide the most robust and compelling insight into the past deposition of Hg across the Arctic.

### 2.7.1. Lake sediments

Lake sediments collectively tell a compelling story about the accumulation of Hg from the long-range transport of Hg emitted by human activities outside the Arctic, to local sensitive environments in the Arctic. When evaluating lake sediments (and any other archive), it is important to examine the chronology and the way it was determined. For example, the dating models employed to obtain a chronology rely on

an estimation of excess  $^{210}\text{Pb}$  activity which may be based on subtracting a background level, rather than measuring supported  $^{210}\text{Pb}$  separately.

Landers et al. (1998), as well as Lockhart et al. (1998), Bindler et al. (2001a), Outridge et al. (2007), Lindeberg et al. (2007) and Muir et al. (2009), reported pre-industrial Hg fluxes in a combined total of 57 Arctic and sub-Arctic lakes (north of  $53^\circ\text{N}$ ) ranging from 0.7 to 54  $\mu\text{g}/\text{m}^2/\text{y}$  (geometric mean 6.7  $\mu\text{g}/\text{m}^2/\text{y}$ ), and 'post-industrial' (around 1960 to late 1990s) fluxes ranging from 2.3 to 52  $\mu\text{g}/\text{m}^2/\text{y}$  (geometric mean 13.9  $\mu\text{g}/\text{m}^2/\text{y}$ ). Increases of Hg flux in recent decades were observed in 53 of 57 cores. In some cases the results were corrected for particle focusing (Lockhart et al., 1998) but not for other processes such as increased sedimentation. Anthropogenic Hg inputs to the lakes ( $\Delta F = \text{recent flux} - \text{pre-industrial flux}$ ) were presented by these authors or have been calculated from their published data.  $\Delta F$  ranged from -14 to 35  $\mu\text{g}/\text{m}^2/\text{y}$  (geometric mean 7.4  $\mu\text{g}/\text{m}^2/\text{y}$ ). Latitudinal and longitudinal trends of  $\Delta F$  for the 57 lakes are shown in Figure 2.23.  $\Delta F$  declined weakly with latitude ( $\log \Delta F$  vs latitude;  $r^2 = 0.10$ ,  $p = 0.015$ ) but was not significantly correlated with longitude.

Recent studies have examined the various factors influencing Hg profiles in Arctic lake sediments. Much of the emphasis has been on the effect of historical variations in sedimentation rates estimated by dating the cores using  $^{210}\text{Pb}$ . Understanding this variation is critical to assessment of Hg fluxes and therefore key findings from recent papers are briefly summarized here. Fitzgerald et al. (2005) found that whole-lake Hg sedimentation determined from 15  $^{210}\text{Pb}$ -dated cores from five small Alaskan lakes (north of the tree line), showed a 3-fold increase in atmospheric Hg deposition since the start of the Industrial Revolution. They concluded that between 11% and 64% of Hg in recent sediments was from soil erosion and that another source term was needed to balance the erosional and sedimentation sinks. They noted that the additional flux needed ( $1.21 \pm 0.74 \mu\text{g}/\text{m}^2/\text{y}$ ) was similar in magnitude to direct wet Hg deposition. They suggested that the missing input may be some combination of springtime Arctic depletion and more generalized deposition of reactive gaseous Hg species. Outridge et al. (2005b) found significant correlations between Al and Hg in the DV-09 (Devon Island Canada) post-1854 stratigraphy and attributed a significant fraction of Hg input to local geological sources via weathering and runoff. Lindeberg et al. (2007) found that large fluctuations in Hg concentrations in pre-19th century sediments of lakes in West Greenland were related to changes in the influx of material from regional aeolian activity. Muir et al. (2009) also found higher recent sedimentation rates in 16 of 31 Arctic and sub-Arctic lakes. They concluded that the increased sedimentation did not appear to have a large lithogenic component (i.e. from erosion or aeolian inputs), because concentrations of lithogenic elements Al and Zn were not correlated with sedimentation rate. The higher recent sedimentation rates could also be due to the flattening of the slope of the  $^{210}\text{Pb}$  activity profile near the sediment surface due to bioturbation or to diagenetic dilution of the  $^{210}\text{Pb}$  due to accumulation of iron oxides at the surface (Gubala et al., 1990). Fitzgerald et al. (2005) noted iron oxide enrichment at the surface in their cores but Muir et al. (2009) found that iron concentrations were positively correlated with sedimentation rate in only 4 of 31 Arctic and sub-Arctic lakes.

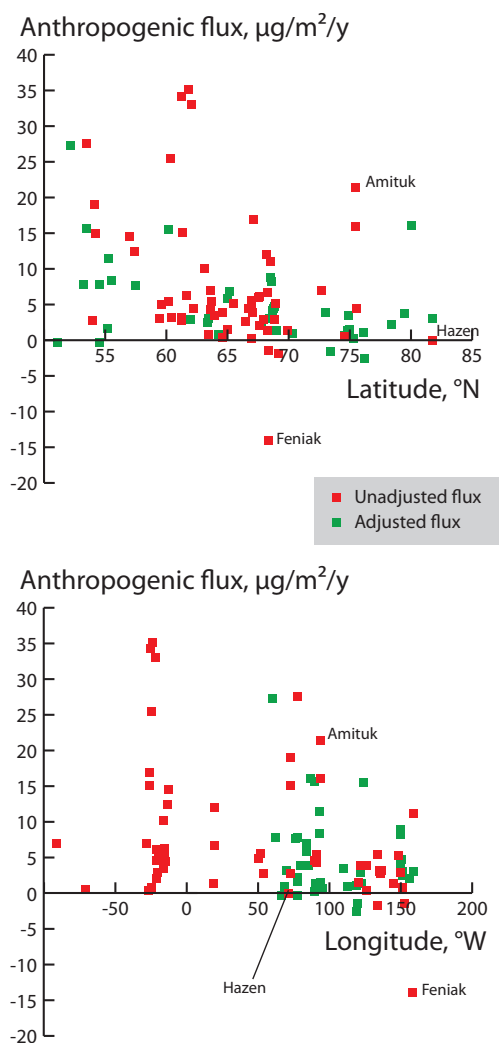


Figure 2.23. Anthropogenic fluxes ( $\Delta F$ ) of mercury in dated sediment cores from Arctic and sub-Arctic lakes. Unadjusted fluxes are from results presented by Landers et al. (1998), Lockhart et al. (1998), Bindler et al. (2001a), Outridge et al. (2007) and Lindeberg et al. (2007). Adjusted fluxes ( $\Delta F_{adj}$ ) are from Fitzgerald et al. (2005), Landers et al. (2008) and Muir et al. (2009).

To adjust for effects of erosional inputs on Hg fluxes, Fitzgerald et al. (2005) and Landers et al. (2008) adjusted Hg fluxes using Mg and Ti, respectively, while Muir et al. (2009) adjusted for sedimentation rate as described by Perry et al. (2005). These adjusted anthropogenic fluxes for 39 lakes ( $\Delta F_{adj}$ ) are plotted with latitude and longitude in Figure 2.23.  $\Delta F_{adj}$  ranged from -2.6 to 27  $\mu\text{g}/\text{m}^2/\text{y}$  (geometric mean 4.5  $\mu\text{g}/\text{m}^2/\text{y}$ ) and declined weakly with latitude ( $\log \Delta F_{adj}$  vs latitude;  $r^2 = 0.17$ ,  $p = 0.01$ ) but not with longitude. These adjusted fluxes apply only to Arctic Canada and Alaska because there are no comparable data available for the rest of the circumpolar Arctic.

Whether adjusted or unadjusted fluxes are used, the geographic trends based on the lake sediment record suggest relatively uniform flux patterns of Hg in Arctic regions (Figure 2.23). In North America,  $\Delta F_{adj}$  is predicted to decline from about 6  $\mu\text{g}/\text{m}^2/\text{y}$  at 60° N to 0.5  $\mu\text{g}/\text{m}^2/\text{y}$  at 83° N. By comparison, the GRAHM model predicted Hg depositional fluxes ranging from about 9.5 to 2.2  $\mu\text{g}/\text{m}^2/\text{y}$  over this latitude range (from 60° to 83° N) in the Canadian Arctic, thus apparently corroborating the lake sediment data (Muir et al., 2009). The Danish Eulerian

Hemispheric model (DEHM) predicted annual Hg deposition with AMDEs included ranging from 12 to 6  $\mu\text{g}/\text{m}^2/\text{y}$  in the Canadian Arctic Archipelago (Christensen et al., 2004). Thus, there is relatively good agreement between the spatial trends of modeled terrestrial Hg fluxes and (measured) anthropogenic fluxes to freshwaters. This modeled result is in the same relative magnitude of Hg flux measured in peat from southern Greenland and around the Faroe Islands (Shotyk et al., 2003, 2005b). However, as DEHM does not presently account for re-emission after AMDEs, further model development is required to determine the degree to which DEHM can be used to support the notion that models are matching observed spatial trends.

The role that climate change has played in modifying Hg fluxes into lake sediments has been an area of recently active research. Two of the possible mechanisms by which this climatic influence may be exerted include increasing algal scavenging of Hg which increases the rate of Hg transfer from the water column to sediments, and inputs of Hg from thawing of adjacent permafrost peatlands. Rydberg et al. (2010) reported that during warm periods in pre-industrial times, Hg export from a thawing sub-Arctic mire in northern Sweden significantly increased Hg flux into an adjacent lake. The impact of the thawing peatland on sedimentary Hg fluxes was as large as that of airborne anthropogenic Hg deposition in the 20th century. Large increases in algal productivity have occurred over recent decades in Arctic lakes (Gajewski et al., 1997; Michelutti et al., 2005). There is evidence that these increases may have markedly increased the rate of organic particle scavenging and transfer of Hg into lake sediments (Outridge et al., 2005b, 2007), in a process analogous to the well-established phytoplankton 'biological pump' for vertical Hg flux in oceans (Cossa et al., 2009; Sunderland et al., 2009). To date, significant Hg-algal carbon flux and/or concentration relationships (with correlation  $r^2$  values  $>0.75$ ) have been found in all four of the lakes (Amituk, DV-09, Kusawa, Hare Indian Lake) which have been investigated in this way (Outridge et al., 2007; Carrie et al., 2010; Stern et al., 2009). It was estimated for Kusawa Lake, Yukon, and Lake DV-09 on Devon Island, Nunvut, that because of this climate-related effect no more than 22-29% of the 20th century increase in Hg concentrations was attributable to anthropogenic Hg inputs (Outridge et al., 2007; Stern et al., 2009). These recent findings, although requiring further investigation and testing, have implications if lake sediments are used to test the validity of atmospheric models.

Sediment total organic carbon (TOC) has occasionally been used to normalize Hg concentrations because it is assumed that most Hg enters lake sediments associated with organic matter. Bindler et al. (2001a,b) and Lindeberg et al. (2006) found that TOC increased over time in dated cores from West Greenland, and Muir et al. (2009) found that TOC increased over time in nine of 31 Canadian Arctic and sub-Arctic lakes. However, Bindler et al. (2001a,b) found that total carbon-normalized Hg concentrations still showed comparable increases in the Hg concentration of recent sediments, indicating that the Hg increases were not related to changes in the total carbon content of the sediment. On the other hand, total carbon data may not be an appropriate measure of the labile, thiol-rich algal organic matter which is believed to be involved in Hg scavenging. Organic matter is a biochemically complex material. Outridge et al. (2005b, 2007) reported increasing TOC in Amituk Lake, and

Lake DV09, but that the relative increase in algal-derived carbon, using a kerogen carbon parameter ('S<sub>2</sub>'), was markedly greater – 760% since 1854. These S<sub>2</sub> carbon increases were highly correlated with diatom valve abundances, suggesting good preservation of the historical organic matter. The increased TOC could be partly due to greater autochthonous organic carbon production or other production in the littoral zone of the lake, as primary production in the littoral zone of lakes is densely concentrated in a considerably narrower space than that in the pelagic zone (Nozaki, 2002). Smol et al. (2005) and Michelutti et al. (2005) have also documented increased production in the pelagic zone. Progressive loss of carbon following burial, as shown by Gälman et al. (2008) for varved lake sediment in northern Sweden is another process that could generate the increase in TOC profiles in recent horizons. However, based on careful characterization of the organic matter using organic geochemistry and petrographic techniques, as well as the agreement between trends in Hg and in diatom abundances, decomposition is unlikely to explain the similar down-core profiles of algal carbon and Hg in the Arctic and sub-Arctic lakes studied by Outridge et al. (2005b, 2007), Carrie et al. (2010) and Stern et al. (2009). Other algal productivity indicators, such as total diatom valve abundance, and total pigment and biogenic silica concentrations, corroborate the occurrence of profound, widespread Arctic lake productivity increases as a consequence of earlier melting and ice-out under warming conditions (Gajewski et al., 1997; Michelutti et al., 2005; Smol et al., 2005).

### 2.7.2. Glacial ice

The state-of-the-art regarding records in glacial ice is the Faïn et al. (2009b) article on the trends in atmospheric levels of GEM in northern latitudes, reconstructed from the interstitial air of firn at Summit, Greenland. The study found that GEM concentrations increased rapidly from ~1.5 ng/m<sup>3</sup> after the Second World War, reached a maximum of about 3 ng/m<sup>3</sup> around 1970, and then decreased until stabilizing at about 1.7 ng/m<sup>3</sup> by around 1995 until the end of the record at 2003 (Figure 2.24b). The later part of their reconstruction agreed with instrument-based measurements of stable GEM concentrations in the Arctic since 1995 (e.g., at Alert; Temme et al., 2007). Overall, the ice core record matched the general trend in estimated global atmospheric emissions and global industrial Hg use (Figure 2.24a). The post-1970 decline in GEM at Greenland Summit was corroborated by coincident and significant declines in particulate Hg concentrations during summer and autumn at Resolute, Nunavut (Li et al., 2009). Spring particulate Hg levels also declined during those three decades, but the decline was not statistically significant because of high intra-seasonal variability possibly related to AMDEs (Li et al., 2009). Readers are cautioned not to place too much emphasis on industrial Hg production figures as a 'surrogate' for atmospheric emissions. The former are based on mining / production statistics and do not (generally) take into account that this has to some extent been offset by recovery / re-use of Hg. For example, cinnabar mines may cut production on a tonne-for-tonne basis as Hg recovered from EU chlor-alkali plants is brought back into circulation. Major atmospheric sources such as coal burning, which are unrelated to industrial Hg uses, add to the difficulty in making direct interpretations (see Section 2.2, for more information). Also, the 1980 global

anthropogenic emissions data shown in Figure 2.24a may be an uncertain estimate, although emissions were almost certainly higher than in the 1990s and 2000s (Pacyna et al., 2006; see Section 2.2).

The atmospheric Hg trend results reported from the Greenland ice core and Resolute airborne aerosols are not consistent with the lake sediment Hg profiles in the Canadian Arctic and sub-Arctic after 1970 (see Figure 2.24). The trends move in opposite directions: declining significantly in air, and rising several-fold in sediment profiles relative to 1900-1910. Section 2.2 discusses changes in global emissions from 1990 to 2005. Global emissions are changing regionally, with relatively greater outputs from Asia during the past 20 years (Pacyna et al., 2006). However, it is unclear how polluted Asian air masses might impact on Hg levels in Canadian Arctic lake sediments, but not in the coinciding Canadian and Greenland atmosphere, particularly when the atmospheric study sites bracket the triangular region of Arctic lake sediments – Resolute (Li et al., 2009) to the west, Greenland (Faïn et al., 2009b) to the east, and Alert (Temme et al., 2007) to the north.

After reviewing the lake sediment- and peat-based Hg literature, Biester et al. (2007) stated that lake sediments appear to be a more reliable archive for estimating historical Hg accumulation rates than peat. This conclusion is not yet generally accepted across the scientific community, although there are many highly cited studies of Hg in lake sediments in the Arctic. However, what seemed (as recently as a few years ago) like very compelling interpretations from Arctic lake sediment studies with respect to their ability to reproduce Hg emission and deposition trends, must now be questioned in the light of recent evidence about the apparent effects of warming perturbing sedimentary Hg records. How these records in lake sediments are now interpreted, particularly given the contradictory atmospheric data from Faïn et al. (2009b), Li et al. (2009) and Temme et al. (2007) is an issue of ongoing debate. From examining the body of literature, scientific consensus has not yet been reached as to whether lake sediments do or do not accurately represent atmospheric Hg deposition in the Arctic, or which models best reproduce historical Hg accumulation.

### 2.7.3. Marine sediments

There have been few additional studies on records in marine sediments since that by Gobeil et al. (1999). The crucial factors governing surface Hg enrichment in Arctic basin sediments were shown to be diagenesis related to the low sedimentation rates (<1 cm ka<sup>-1</sup>) and sediment mixing rates (<0.03/cm<sup>2</sup>/y) which redistributed Hg in the sediment profile. In all seven cores they investigated, strong similarities were observed between the Hg and reactive iron (Fe) profiles, implying that a proportion of the total Hg deposited is recycled along with Fe during redox changes. Intense redox processing in these cores was demonstrated by sharp decreases in organic content with depth and by vertical profiles showing surface enrichment of reactive elements. Thus, Gobeil et al. (1999) demonstrated that because of post-depositional processes, Arctic marine sediment archives are not generally reliable archives of Hg deposition.

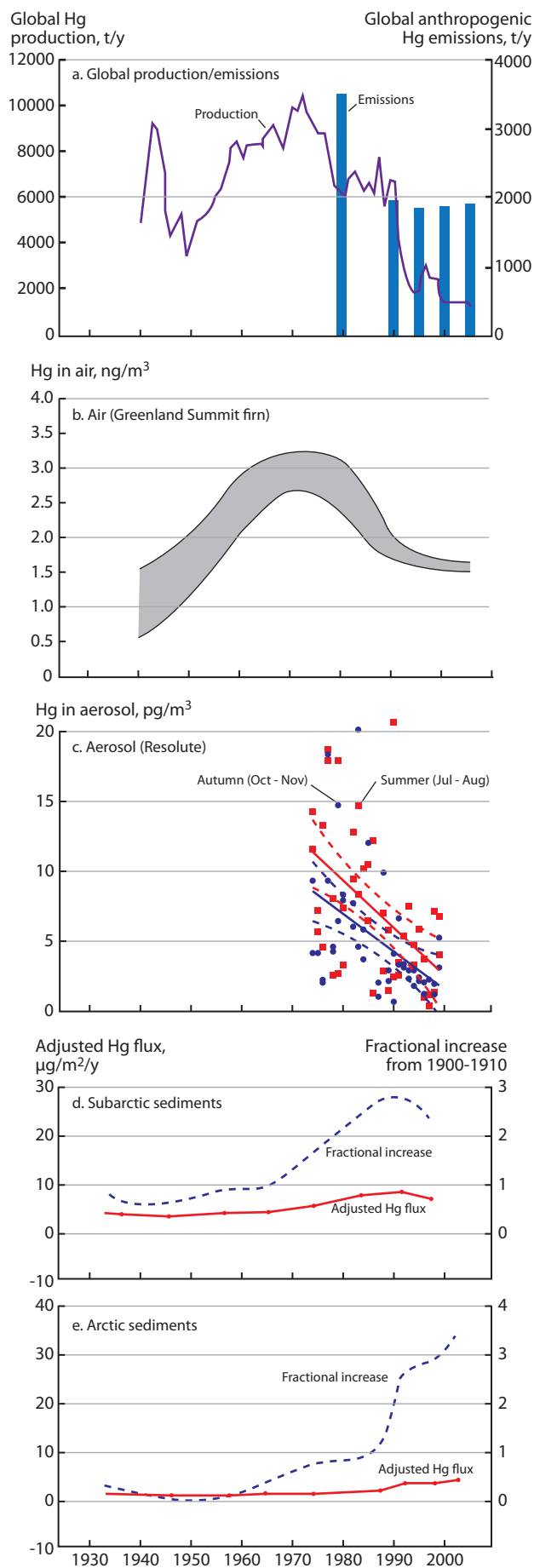


Figure 2.24. Comparison of published trends since 1940 in (a) global industrial mercury production (line; USGS, 2006) and global atmospheric emissions (bars; 1980 – Nriagu and Pacyna (1988), 1990 to 2005 – this report Section 2.2.2), (b) gaseous elemental mercury concentrations in Greenland Summit firn (Fain et al., 2009b), (c) aerosol mercury at Resolute (Li et al., 2009), and in (d) Canadian sub-Arctic and (e) Arctic lake sediments (Muir et al., 2009).

### 2.7.4. Peat bogs

While ombrotrophic peat bogs are widely accepted as reproducing the atmospheric deposition of Hg (e.g., Steinnes and Sjobakk, 2005; Farmer et al., 2009) and there is good agreement between the measured accumulation rates and the modeled rates for lead (e.g., von Storch et al., 2002), the case is not as straightforward for Hg in peat types other than ombrotrophic deposits. Further complications arise when considering peat bogs subject to freeze-thaw cycles and other physical and chemical processes specific to the Arctic. The Biester et al. (2007) review started a debate in the environmental archive community regarding the overall validity of peat archives of Hg, especially those in the Arctic (see Givelet et al., 2004b; with subsequent critical comment and response: Bindler et al., 2005; Shoty et al., 2005a). Studies of the historical Hg record in peat bogs suggested higher modern increases (9- to 400-fold, median 40-fold) than in lake sediments. Biester et al. (2007) compared published data of background and modern Hg accumulation rates derived from globally distributed lake sediments and peat bogs and discussed reasons for the differences observed in absolute values and in the relative increase in the industrial age. Direct measurements of modern wet Hg deposition rates in remote areas of the Northern Hemisphere presently coalesce around the range of about 1 to 4 µg/m²/y, but were possibly as high as 20 µg/m²/y during the 1980s. Values on the same order of magnitude were determined from lake sediments, thus suggesting that modern Hg accumulation rates derived from peat bogs tended to overestimate deposition. Biester et al. (2007) attributed this to the smearing of <sup>210</sup>Pb in the uppermost peat sections and thus an underestimation of peat ages, and attributed the lower background Hg accumulation rates in peat as compared to lake sediments to non-quantitative retention and loss of Hg during peat diagenesis. Both points are contentious given the reliable Pb isotopic profiles retrieved from peat bogs as well as the lack of association between direct measures of peat humification and Hg accumulation rates (Shoty et al., 2005b; Zaccone et al., 2009).

### 2.7.5. Summary comments on records in environmental archives

At least in part, the lack of agreement concerning the reliability of environmental archives is due to difficulties in establishing reliable chronologies, and in the present limits of geographical coverage of most archive types. Reconstructing archive data requires a reliable chronology of the archive. Producing this chronology is not trivial and generally this is one of the sources of uncertainty when interpreting the archive. Another source is the lack of geo-spatial coverage. Each archive type represents the transfer of Hg by various processes from the atmosphere to its ultimate deposited form, where at least a proportion of

the original deposited amount is ultimately preserved. The transfer functions from air to ultimate accumulation in an archive, and the subsequent post-depositional processes, are still not well described in any of the archives, although there have been positive efforts to model the ultimate fate of Hg in a lake (Gandhi et al., 2007; Knightes et al., 2009). Post-depositional processes are likely to account for some of the non-correlation observed between the measured trends in archives and the modeled values.

The only historical environmental archives of Hg with enough data to reasonably statistically compare the results with the models, besides the ice cores, are the lake sediments. There are simply not enough studies in peat to reliably test for a compelling correlation. Nevertheless, additional studies in all archives are needed as the historical records may reflect different air masses and terrestrial catchments.

Although the number of studies of environmental archives has increased and systematically attempted to address known scientific gaps, there are still significant gaps that must be investigated to allow these past records of Hg deposition to be effectively used to help parameterize models to predict future concentrations in the various environmental archives. The answer to the question *Can atmospheric fate models reproduce historical Hg deposition rates recorded in sediments, peat or by instruments?* based on the available peer reviewed literature and state of the art is *a qualified yes*. The recent ice records are presently providing the most unequivocally reliable records with an excellent correlation between the measured trends and global anthropogenic emission records, but there is not yet a consensus among the authors of the present report as to whether lake sediments do or do not accurately represent rates of atmospheric Hg accumulation in the Arctic.

## 2.8. Conclusions and recommendations

Conclusions (in numbered bullets) are organized under section headings, followed by recommendations in italics when appropriate.

### What are the current rates of global anthropogenic emissions of mercury to air?

1. Recent inventories of the global anthropogenic emissions of Hg to air for 2005 indicate annual emissions of 1921 tonnes. Emissions occur both from 'unintentional' sources (i.e., where Hg is present as a contaminant in fuels and raw materials) and from intentional use of Hg. Stationary combustion is the largest single source sector at 880 tonnes, mainly from the use of coal for energy production and thus also the largest 'unintentional' source. Artisanal gold production is the second largest source at 330 tonnes and also the largest intentional use source. Metal production and cement manufacturing are also large contributors to the global emissions.
2. Asia is by far the region with the largest emissions of Hg to air with about 65% of the total emissions, followed by North America and Europe.
3. A reanalysis of global emission inventories from 1990 to 2000 has produced a new set of consistent emissions data.

The analysis shows that global emissions have been fairly constant during the period 1990 to 2005. During this period, emissions have decreased in Europe and North America but have increased in Asia. The re-analysis also includes an estimate of emissions from intentional use of Hg for the same period.

4. Once released to the environment, Hg can be recirculated between different compartments. Re-emissions of Hg to air will occur via evasion from natural surfaces (water, snow, soil, vegetation) as well as anthropogenically induced emissions via, for example, biomass burning.
5. Natural emissions result from the presence of Hg in the Earth's crust and can occur from, for example, volcanoes or soils enriched in Hg-containing minerals. Once released, naturally emitted Hg is indistinguishable from anthropogenic Hg and will follow the same atmospheric pathways i.e. transport, transformation, deposition and re-emissions from natural surfaces.
6. Available estimates of natural and re-emissions are within the range 2000 to 5000 tonnes per year and are thus of the same magnitude or larger than anthropogenic emissions. For modeling of atmospheric transport and for assessment of environmental contamination it is thus necessary to include these fluxes.

*For assessment of global transport and impacts of Hg and for the development of strategies for reducing the impacts, it is necessary to reduce the uncertainty of emission inventories. Information on Hg contents in fuels and raw materials as well as information on the current technical status of industrial sectors is lacking. Emission estimates from some sectors notably intentional use and waste handling are associated with large uncertainties and need to be better characterized.*

*Estimates of natural emissions and re-emissions are often based on a very limited number of measurements and models using a mass balance approach. Further research into the transfer of Hg from different environmental compartments to air is a high priority.*

### Are natural sources significant contributors of mercury to the Arctic environment?

7. Despite the absence of any known natural sources within the Arctic, natural emissions of Hg to air are estimated to contribute between 1000 to 2000 tonnes per year globally and are thus an important factor in the global atmospheric cycling of Hg including deposition to the Arctic.

### What are the relative importance of and processes involved in atmospheric, oceanic, riverine and terrestrial inputs of mercury to the Arctic?

8. The main input source of Hg to the Arctic is the atmosphere, which contributes slightly less than half of the annual input. Oceanic transport mainly from the Atlantic makes up around 23% as does erosion. The remaining fraction originates from riverine input.

### What is the influence of mercury speciation on total mercury transport by air?

9. Atmospheric chemistry and changes in speciation are key processes determining the transport of Hg from global sources to the Arctic and other remote ecosystems. The bulk of the atmospheric Hg is in the form of elemental Hg vapor which can be oxidized to form divalent forms which are more water soluble and thus more prone to deposition via wet or dry processes. Divalent gaseous Hg is often operationally defined as RGM (reactive gaseous mercury) or GOM (gaseous oxidized mercury).
10. RGM is formed continuously in the troposphere via reactions between elemental Hg and oxidants such as OH and Br. The exact reaction mechanisms are somewhat uncertain mainly due to experimental difficulties in determining reaction rates and product formation.
11. Operationally defined measurement techniques for RGM have been extensively applied in the Arctic for measurements of atmospheric mercury depletion events (AMDEs), where a very rapid oxidation of Hg occurs during the Arctic spring. These AMDEs lead to deposition of Hg from the atmosphere. In subsequent photochemically induced reactions, a fraction of the oxidized Hg can be reduced back to the elemental form and volatilized to the atmosphere again.
12. An analysis of long-term measurement data of atmospheric Hg in the Arctic indicates stable conditions. A slight decrease has been observed in Alert (Canada), but results from other sites do not show any significant trends.
13. Very few time series of atmospheric deposition measurements exist in the Arctic. Bulk deposition data from Pallas (Finland) indicate some variability but no significant trend.

### What is known about the net atmospheric mass contribution of mercury to the Arctic?

14. The transport processes in the Hg models are well represented; these have been developed and extensively evaluated for better known atmospheric chemical species. Model estimates of source attribution of Hg in the Arctic are remarkably consistent, and this provides evidence for the robustness of model dynamics in simulating transport.
15. The model-simulated annual mean GEM concentrations in the Arctic are within a factor of 1.1 of measured values at six monitoring sites. Model estimates of yearly wet deposition differ from measured values at three sites (two sub-Arctic, one Arctic) by a factor of 1.2 to 7.6.
16. Models are generally capable of simulating the depletion / re-emission cycles of Hg during springtime AMDEs in the Arctic, implying the role of halogen photochemistry; however there remains considerable uncertainty in Hg chemical kinetics parameters in air and at snow surfaces which limits precise determination of net deposition fluxes.
17. The most recent estimates of the net deposition of atmospheric Hg to the Arctic (north of 66.5° N) are provided

by the four Hg models presented in this report. The model net deposition estimates range from 80 to 143 tonnes per year with a mean value of 116 tonnes per year. Net deposition is found to be highest in the region north of Europe and lowest in the region north of North America. Maximum net deposition is found to occur in the months of March, April and May and is attributed to enhanced deposition during AMDEs. The model mean net deposition during spring (March to May) is 42.8% of the yearly net deposition.

18. Anthropogenic emissions, terrestrial emissions (natural and revolatilized) and oceanic emissions (natural and revolatilized) each contribute approximately one third of the total deposition to the Arctic. The total deposition contribution (anthropogenic, natural, revolatilized) is highest from East Asia (21.4%), followed by Europe (8.7%), Africa (7.4%), North America (7%), South Asia (5.7%), Australia and Oceania (5.4%), South America (5%) and Central Asia (includes Russia) (4.6%). The contribution from anthropogenic sources alone is highest from East Asia (13.6%), followed by Europe (4.8%), Central Asia (includes Russia) (2.6%), North America (2.2%), South Asia (2.2%), Australia and Oceania (1.5%), South America (1.4%) and Africa (1%). The anthropogenic source attributions of Hg deposition to the Arctic estimated by different models are very close, and more reliable compared to the non-anthropogenic source attributions.
19. Geographic distribution of the Hg contributions to the Arctic from major emission source regions shows small but definite correlation with the direct transport pathways; a result of long lifetime (6 to 24 months) of elemental Hg in the atmosphere. The North American and East Asian emissions impact is somewhat higher in the western hemisphere, whereas the South Asian impact is slightly higher over Greenland and the adjacent ocean. The contribution from European sources has the strongest regional variability. These results suggest that relative changes in global emissions from these regions have a small differential impact on the atmospheric deposition rates in the Arctic.
20. Changes in anthropogenic global emissions between 1990 and 2005 led to generally corresponding changes in deposition to the Arctic. However, the impact of emissions reductions in Europe and North America is found to be larger compared to the impact of increases in emissions in other regions between 1995 and 2000. The smallest changes in deposition are simulated for the sub-Arctic and Arctic regions north of North America and the largest changes are found for the sub-Arctic and Arctic regions north of Europe. These regional differences are attributed to the relatively larger impact of East Asian emissions to the Arctic region of North America and the larger impact of European emissions to the Arctic region north of Europe.
21. There are significant differences between current Hg model configurations, most notably in natural and revolatilized Hg emissions, chemical mechanisms and reaction rate constants. The models represented in this report cover a comprehensive range of uncertainties in Hg emissions and processes found in the literature. Therefore the results reported here provide

a reasonable estimate of the uncertainty in the current ability to determine the atmospheric Hg input to the Arctic using models.

*Model estimates of the source attribution and temporal trends of Hg in the Arctic depend highly on the reliability of anthropogenic emissions data and on the speciation of Hg emissions. Therefore, further improvements of global Hg emission inventories are needed.*

*Studies are required for quantitative and mechanistic understanding of natural and revolatilized Hg emissions from various surfaces (soils, water, snow, vegetation) for constraining the models uncertainties.*

*Improved understanding of Hg chemical mechanisms, reaction rates and products in gas, aqueous and heterogeneous phases in global and Arctic environment is needed through laboratory and field measurement studies. Better understanding of bromine reaction rate constants in air and Hg reduction chemistry in snow are of particularly importance for the Arctic.*

*The models are generally consistent with each other for quantities that are better measured such as GEM, however the differences are large for quantities lacking observations such as wet and dry deposition in the Arctic. Measurements over the Arctic basin are largely missing which severely restricts the evaluation of the models over the Arctic Ocean. There is a need for a comprehensive network of measurements in the Arctic that includes concentrations of speciated Hg and chemical reactants in air, as well as wet and dry deposition.*

*Modelers need to explore the use of surface measurements such as Hg concentrations in snowpacks, streams and sediments to constrain the models.*

*Comprehensive parameterizations for Hg exchange between air and cryosphere need to be developed to limit the uncertainty in net deposition estimates to the Arctic.*

*Although, the atmospheric reservoir of mercury is comparatively much smaller, the atmosphere serves as an efficient mechanism for exchanging Hg between the two large reservoirs of Hg in the terrestrial and oceanic systems. Biogeochemical models linking atmosphere, ocean and terrestrial systems are needed to take into account the entire cycling of Hg in the environment for an adequate assessment of Hg inputs to the Arctic. It is particularly relevant for the evaluation of long-term trends, future scenarios and the impact of climate change on Hg pollution in the Arctic.*

*Modeling studies are needed to investigate the impact of changes in meteorology, atmospheric chemical composition, land-use and climate on Hg budgets in the Arctic.*

### **Can atmospheric fate models reproduce historical mercury deposition rates recorded in sediments, peat or by instruments?**

22. Reconstructing archive data is restricted due to difficulties in establishing reliable chronologies, and in the present limits of geographical coverage of most archive types. The transfer functions from air to ultimate accumulation in an archive, and the subsequent post-depositional processes, are still not well described in any of the archives. Additional studies in all archives are needed as the historical records may reflect different air masses and terrestrial catchments.

23. The answer to the section question is a *qualified yes*, based

on the available peer reviewed literature and state of the art. The recent ice records are presently providing the most unequivocally reliable records with an excellent correlation between the measured trends and global anthropogenic emission records, but there is not yet a consensus among the authors of the present report as to whether lake sediments do or do not accurately represent rates of atmospheric Hg accumulation in the Arctic.

*It is possible that precipitation type as well as amount may be an issue in relation to the model calculations. The relative scavenging effect of snow vs rain on the flux of atmospheric Hg is a research area needing attention.*

*Sampling both dry and wet deposition under Arctic conditions is an important area requiring further research and development; sampling snowfall is a particular challenge in this respect. These measurements are important for improved parameterization of models.*

*Depositional and flux measurement techniques and campaigns are needed as wet deposition may be similar at different times and locations yet re-volatilization may be quite different.*

*It is of the utmost importance that better techniques be developed for measuring the geographical and temporal dynamics of Hg deposition and the concomitant re-emission of atmospheric Hg to the Arctic and the rest of the World. Because of the global cycling of Hg it is not possible to develop an accurate model of the Arctic portion of the global cycle in regional isolation. Therefore, technological development of measurement techniques is needed so that the concentrations of Hg species in the atmosphere can be measured rather than only the fractionation of Hg. Furthermore, there is only one published study of the fluxes of RGM and a few studies of the fluxes of GEM in the Arctic.*

*Further studies to investigate the possible over-estimation of atmospheric wet deposition fluxes by lake sediments and atmospheric models, and the reasons for any over-estimation are needed. These studies must be corroborated with studies of Hg in annually deposited snow and ice where possible, using uniformly agreed sampling and analysis methods.*

*One of the gaps in knowledge for future studies is the need to develop and accept common sampling and dating routines, as best practice, to allow better intercomparison of the data sets.*

*AMAP should recommend the creation of an expert working group to address the question of exactly what studies and data are needed ensure that the models are properly parameterized to predict the future deposition and likely re-emission of Hg and its ultimate fate in future Arctic ecosystems.*

*There is a need for standardized best practices for sampling and later biogeochemical analysis in environmental archives, as such protocols do not exist in the literature except for peat (see Givelet et al., 2004a). Studies presenting Hg as stand alone data generally therefore do not advance overall understanding.*